Title
Telomerase Holoenzyme Proteins and Processivity Subunit in Tetrahymena thermophila

Author
Min, Bosun

Publication Date
2009

Peer reviewed|Thesis/dissertation

Telomerase Holoenzyme Proteins and Processivity Subunit in *Tetrahymena thermophila*

by

Bosun Min

B.A. (University of California, Berkeley) 2002

A dissertation submitted in partial satisfaction of the

requirements for the degree of

Doctor of Philosophy

in

Molecular and Cell Biology

in the

Graduate Division

of the

University of California, Berkeley

Committee in charge:

Professor Kathleen Collins, Chair
Professor Donald Rio
Professor Tom Alber
Associate Professor Eva Harris

Fall 2009

The dissertation of Bosun Min is approved:

Chair _____ Date _____

_____ Date _____

_____ Date _____

_____ Date _____

University of California, Berkeley

ABSTRACT

Telomerase Holoenzyme Proteins and Processivity Subunit in *Tetrahymena thermophila*

By

Bosun Min

Doctor of Philosophy in Molecular and Cell Biology

University of California, Berkeley

Professor Kathleen Collins, Chair

Telomeres are specialized protein-DNA structures that protect the ends of linear chromosomes, and they are maintained by the telomerase ribonucleoprotein (RNP) enzyme complex. Recombinant telomerase RNP with catalytic activity contains, at a minimum, the catalytic reverse transcriptase subunit (TERT) and the telomerase RNA (TER). However, endogenous telomerase is a much larger holoenzyme complex, with telomerase-associated subunits that contribute to RNP assembly and regulation. Telomerase-associated subunits may also directly affect the biochemical features of telomerase catalytic activity. *In vitro* reconstitution of *Tetrahymena thermophila* minimal RNP results in telomerase activity with low repeat addition processivity (RAP), while the endogenously assembled complexes can have both low and high RAP.

Knowledge of a comprehensive list of telomerase-associated proteins expands our understanding of how telomerase-associated proteins regulate telomerase. Therefore, I optimized an affinity purification of TERT-associated proteins and identified telomerase-associated proteins to add to the list of known subunits. I have also begun characterizing

the architecture of the telomerase holoenzyme: three subunits form a subcomplex that bridges the minimal RNP and a processivity factor, which contains telomeric single-stranded DNA-binding activity. With these telomerase subunits, a telomerase complex with high RAP can be reconstituted *in vitro*. The work described here expands the known functions of telomerase-associated proteins and the molecular mechanisms of telomere length regulation.

Committee Chair _____

ACKNOWLEDGMENTS

I would like to thank everyone who made this thesis possible. First and foremost, Kathy Collins, who guided me through my graduate career and taught me so much. My thesis committee not only provided feedback about my scientific progress but also encouraged me to think about my future career.

Collins lab provided a scientifically nurturing environment. I have had the pleasure of learning from, working with, and helping train many Collins labbites: Judy Wong, Quinton Tieu, Rama Prathapam, Bobby Hogg, Dragony Fu, Catherine O'Connor, Suzanne Lee, Sharlene Lim, Mary Couvillion, Tim Errington, Aaron Robart, Emily Egan, Kristin Talsky, Alec Sexton, Kasper Andersen, Barbara Eckert, and Kyungah Hong. They enriched my graduate experience. Extra thanks to my former and current baymates (Shar and Mary).

My family gave endless support and made it possible for me to be where I am now. I especially want to thank Kent Hu, my better half, for always being there for me.

TABLE OF CONTENTS

CHAPTER ONE

Telomerase Complexes, Telomere Complexes, and Telomerase Recruitment to Telomeres

Telomeres are specialized chromatin structures found at the ends of linear chromosomes. In most eukaryotes, they are made up of simple G-rich repeats in the strand that makes up the 3' overhang: TTAGGG in vertebrates and TTGGGG in the ciliate *Tetrahymena thermophila*. Telomeres are important for chromosome stability and complete genome replication. Because DNA replication of linear chromosome ends results in sequence loss, the repetitive nature of telomeres ensures that chromosomes only lose repetitive sequences that can be restored. Moreover, telomeres also function in protecting the ends of chromosomes from nucleases and preventing the DNA ends from being recognized as breaks to be repaired (reviewed in (Palm and de Lange, 2008)).

Because telomeres shorten with each round of DNA replication, there needs to be a mechanism to maintain telomeres. Most organisms solve this problem using telomerase, a ribonucleoprotein (RNP) enzyme complex. The catalytic subunit, telomerase reverse transcriptase (TERT), assembles with an RNA subunit (TER). TERT uses the template region of TER to copy G-rich repeats onto the chromosome ends (reviewed in (Cristofari, 2006)). In order to extend telomeres, telomerase needs to access the 3' single-stranded DNA (ssDNA) ends of telomeres. Telomere protective function seems to be at odds with telomerase function, but telomere-binding proteins can dynamically modulate the

chromosome end-protection and chromosome accessibility to telomerase (see discussion below and reviewed in (Bianchi and Shore, 2008)).

Telomerase exists as a multi-protein holoenzyme complex with telomerase-associated proteins that function in RNP biogenesis and telomerase regulation (reviewed in (Collins, 2006)). Several proteins bind TER *in vivo*, accomplishing proper RNP biogenesis. TER-binding proteins help stabilize TER by protecting it from nucleases and by folding the RNA properly. Some are telomerase-specific while others also function in other cellular RNA processing. For example, human TER requires H/ACA proteins for stability, and these proteins continue to associate with the telomerase holoenzyme. Other telomerase-associated proteins affect telomere length maintenance by modulating telomerase recruitment to telomeres, some in collaboration with proteins bound to telomeric DNA. In addition to TER-binding proteins, the budding yeast TERT also associates with Est1 and Est3 proteins, which are part of the telomerase holoenzyme.

The Telomerase Holoenzyme in Tetrahymena thermophila

Telomerase activity was first discovered in *T. thermophila*, a unicellular eukaryote (Greider and Blackburn, 1985). This discovery was greatly facilitated by the relative abundance of telomeres and telomerase molecules. There are ~40,000 telomere ends in a single *T. thermophila* cell. Moreover, cells divide very quickly by fission (~2.5-3 hr doubling time) and telomeres need to be maintained constantly. There are approximately 25,000 molecules of telomerase RNP per cell (Avilion et al., 1992). Therefore, *T. thermophila* is an ideal organism to study the "active" form of a telomerase

holoenzyme in which telomerase activity is positively stimulated by telomerase-associated proteins.

The telomerase holoenzyme complex in *T. thermophila* has been studied through the affinity purification of tagged TERT and TER (Cunningham and Collins, 2005; Witkin and Collins, 2004). Past work in our lab and the work described here provide insight into the telomerase holoenzyme architecture and function. Together with TER, there are eight known telomerase components in *T. thermophila*. The known telomerase-associated proteins are: p133 (TERT), p65, p75, p45, p19, p82, and p50. These telomerase-associated proteins were initially named based on their predicted molecular weight, but some have been renamed after further studies to reflect their known function within the telomerase holoenzyme. This list may not be complete since it is likely that other proteins transiently interact with telomerase *in vivo*. However, our successful *in vitro* reconstitution of telomerase activity, similar to the activity of endogenously assembled telomerase, suggests that we have now identified all the components required to build a telomerase holoenzyme (Chapter Three).

The initial biogenesis of the telomerase RNP involves p65, TER, and TERT. The p65 subunit is a La motif-containing, telomerase-specific protein that binds and stabilizes TER (Prathapam et al., 2005; Witkin and Collins, 2004). Knockdown or overexpression of p65 decreases or increases TER level, respectively (Tieu and Collins, unpublished data) (Witkin and Collins, 2004). *In vitro* studies revealed that p65 binds TER and causes a conformational change in the RNA that facilitates subsequent binding of TERT (Prathapam et al., 2005; Stone et al., 2007). We call the TERT·TER·p65 complex the core

RNP complex since it contains the minimal subunits (TERT+TER) required for catalytic activity and represents an early step in the RNP biogenesis.

Telomerase-associated p75, p45, and p19 subunits assemble as a subcomplex that we named TASC, for Telomere Adaptor Subcomplex. Knockdown of any one of the TASC proteins does not affect TER levels, suggesting that, unlike p65, TASC does not affect telomerase RNP assembly (Min, 2009; Witkin et al., 2007). TASC component knockdown also causes short telomeres, indicating that TASC function is essential for telomerase activity at telomeres. Therefore, TASC likely assembles with the core complex to form a telomerase complex that is required for proper telomere length maintenance.

Knockdown of p82 also causes telomere shortening without changing TER levels, and we found that p82 telomerase subunit assembles with the core complex through its interaction with TASC. Interestingly, the purification of tagged TERT or tagged TASC component co-purifies substoichiometric amount of p82, and the purification of tagged p82 enriches for telomerase complexes with high repeat addition processivity (RAP). Telomerase high RAP activity reflects the low dissociation rate of the telomerase complex from its elongating substrate. I found that p82 is the elusive telomerase anchor site protein that increases telomerase processivity *in vitro* (Chapter Two). We renamed p82 as Teb1 (for Telomere-Binding 1) to better reflect its biochemical properties of binding sequence-specifically to telomeric ssDNA (Chapter Three).

Telomerase holoenzyme complexes are not homogeneous; complexes purified by tagging different components of telomerase in *T. thermophila* co-purify variable amounts of other telomerase subunits. Under native purification conditions, we are examining a

mixed snapshot of telomerase complexes that exist in an asynchronously growing population. Whether these complexes represent steps in assembly, disassembly, or regulation will be elucidated in future studies. In addition, it will be equally important to study the various telomere holoenzyme complexes in the context of the cell cycle and the substrate telomeric chromatin, in order to fully understand telomerase function *in vivo*.

Telomere-Binding Proteins

Telomeres consist of a double-stranded DNA region and, in most cases, a G-rich single-stranded 3' overhang region. The lengths of both dsDNA telomeric region and ssDNA G-strand overhang vary between organisms. Both dsDNA and ssDNA regions of telomeres are bound by sequence-specific DNA-binding proteins, or telomere-binding proteins (TBP), that modulate telomere accessibility. The ssDNA TBPs serve to protect the telomeric ssDNA overhangs from degradation by nucleases and also from being recognized as dsDNA breaks; this is called end protection or telomere capping. TBPs are also important for maintaining proper telomere length and aiding telomere replication.

The first ssDNA TBPs to be identified were TEBP (telomere end binding protein) proteins α/β from the ciliate *Oxytricha nova* (Gottschling and Zakian, 1986; Price and Cech, 1987). The fission yeast and mammalian homologs of TEBP α subunit were named Pot1, for protection of telomeres (Baumann and Cech, 2001). Both TEBP α/β and POT1 contain oligonucleotide/oligosaccharide binding (OB) folds and have high sequence specificity for cognate telomeric ssDNA. In mammalian cells, POT1 interacts with TPP1 (TEBP β homolog) and exists in a multiprotein complex called shelterin that includes dsDNA TBPs (Palm and de Lange, 2008). POT1 homologs were also found in

Arabidopsis thaliana and *T. thermophila* (Jacob et al., 2007; Shakirov et al., 2005). It has not been easy to find all the TBP homologs in the sequenced genomes of other organisms because OB fold structures can be maintained even with great divergence in the primary sequence.

S. cerevisiae does not have a POT1 homolog but relies on end capping by another ssDNA TBP called Cdc13 that forms a complex with Stn1 and Ten1 (reviewed in (Bianchi and Shore, 2008)). Like POT1, Cdc13 binds sequence-specifically to telomeres (Nugent et al., 1996). Originally, it was proposed that instead of a POT1 complex, budding yeast evolved a different complex, called the CST complex (Cdc13-Stn1-Ten1). Budding yeast CST complex caps telomeres, modulates telomerase association with telomeres, and associates with DNA polymerase α/primase (Pol α), the lagging strand polymerase complex. The CST complex may be an alternate capping complex that is used instead of the POT1 complex.

Intriguingly, the fission yeast *Saccharomyces pombe* has both Stn1 and Ten1 homologs in addition to a POT1 complex (reviewed in (Moser and Nakamura, 2009)). Fission yeast Stn1 and Ten1 function in telomere capping: like pot1 mutant, stn1 or ten1 mutant has telomere loss phenotype. Although the Cdc13 homolog has not yet been found, Stn1 and Ten1 do not interact with the POT1 complex. Thus, it was possible that both POT1 and CST complexes coexist in an organism. Recent work in human cells, mice, and *A. thaliana* found Stn1 and Ten1 homologs and Ctc1 (Conserved telomere maintenance component 1) (Miyake et al., 2009; Surovtseva et al., 2009). Ctc1, Stn1, and Ten1 form a complex and localize to telomeres. Ctc1 does not seem to be closely related to Cdc13. However, this complex also functions in telomere replication (and replication

outside of telomeres) and in promoting lagging strand synthesis; in serving this function, Ctc1-Stn1-Ten1 is analogous to the budding yeast Cdc13-Stn1-Ten1 complex. Therefore, the mammalian and plant Ctc1, Stn1, and Ten1 complex is also called the CST complex. In mammals and plants, the POT1 complex is used for telomere capping while the CST complex is used also for telomere replication. On the other hand, budding yeast CST complex serves both functions at telomeres. It is unclear whether fission yeast Stn1 and Ten1 also form a CST complex, but these proteins also function in telomere capping and may overlap with POT1 complex function. Therefore, the complexes that exist at terminal ends of telomeres are more dynamic than previously appreciated.

Regardless of the complex(es) found at telomeres, telomerase is unlikely to encounter naked chromosome ends. In some cases, telomerase is recruited to telomeres by TBPs and TBP-interacting factors. For example, fission yeast Ccq1 (part of the POT1 complex) physically interacts with TERT and the rest of the POT1 complex (Miyoshi et al., 2008). In the budding yeast, Cdc13 (CST complex) positively regulates telomerase by associating with Est1, a telomerase-associated protein. In human cells, Pot1 and Tpp1 (POT1 complex) enhance telomerase activity and may function directly in telomerase recruitment (Wang et al., 2007; Xin et al., 2007). As telomeric chromatin is remodeled during DNA replication, TBP complexes can either positively or negatively regulate telomerase activity by promoting telomerase-accessible or telomerase-inaccessible conformations.

Telomere Replication and Telomerase

Replication of telomeres is carried out by the general DNA replication machinery, as well as by telomerase (reviewed in (Gilson and Geli, 2007a)). Replication fork origins are located within the subtelomeric regions in yeast. In other organisms, particularly those with longer telomeres, replication may also start within telomeres. Replicating the telomeric chromatin can be challenging to the DNA replication machinery; telomeric chromatin can exist in t-loop structures, and the exposed ssDNA G-strand can form G-quadruplex structures (reviewed in (Oganesian and Karlseder, 2009)). T-loops are unresolved D-loop structures formed by the telomeric ssDNA invading the telomeric dsDNA region. G-quadruplexes are structures that can form with G-rich ssDNA wherein the guanines form Hoogsteen interactions and fold into a form that may require helicases to resolve. Both t-loops and G-quadruplexes are structures that likely contribute to the protective function of telomeres but need to be resolved when telomeres are replicated.

Leading strand synthesis of a telomere creates a new G-strand, and lagging strand synthesis creates a new C-strand. Parental C-strand that is paired with the new G-strand must be processed to generate a 3' G-strand overhang. Telomerase is recruited to the G-strand ssDNA to extend the overhangs and prevent progressive telomere shortening, in organisms and cells with active telomerase. Lagging strand synthesis of telomeres by Polymerase (Pol) α is coordinated by TBPs and, in some cases, by telomerase itself. For example, *Euplotes* telomerase physically associates with primase (Ray et al., 2002). In budding yeast, Cdc13 associates with Pol α (Qi and Zakian, 2000), and in human cells, members of the CST complex (Ctc1 and Stn1) stimulate Pol α (Casteel et al., 2009).

Interestingly, the structure of the yeast CST complex is predicted to be similar to the structure of the RPA complex (Gao et al., 2007; Gelinas et al., 2009). Both RPA-like

CST complex and RPA complex are likely to function in telomere replication. RPA is a ssDNA-binding complex made up of RPA1 (70 kDa), RPA2 (32 kDa), and RPA3 (14 kDa). It is the eukaryotic equivalent of SSB (ssDNA-binding protein) that functions in DNA replication (reviewed in (Wold, 1997)). RPA binds the ssDNA that forms during replication initiation and also interacts with Pol α. RPA associates with the replication fork and plays a role in DNA replication elongation; it is also used during DNA recombination and DNA repair.

There are many ways in which RPA may play a role at telomeres. However, because telomere replication is carried out by the general DNA replication machinery, it becomes challenging to separate the role of RPA in chromosome replication and in telomere replication. The *Leishmania* (trypanosome) RPA-1 has been implicated in telomeric ssDNA binding by ChIP and co-localization (Neto et al., 2007). Human RPA unfolds G-quadruplexes *in vitro* and may promote telomerase activity by providing ssDNA substrate (Salas et al., 2006). Depletion of RPA from human cell extracts leads to decrease in telomerase activity that can be reversed by the addition of recombinant RPA; however, excess RPA leads to telomerase inhibition (Rubtsova et al., 2009). In budding yeast, RPA is important for telomerase activity at telomeres (Schramke et al., 2004), but whether this is a direct effect is still unclear. Telomerase access may be modulated by telomere replication as well as by direct recruitment through Cdc13 and Est1 (telomerase-associated protein) association (Chandra et al., 2001).

These results implicate TBPs, general DNA replication apparatus, and telomerase in telomere replication and maintenance. How exactly the recruitment of the lagging strand polymerase is coordinated with telomerase activity remains to be elucidated.

T. thermophila *Teb1: Potential Link between Telomerase and Telomere Replication*

Teb1 shares sequence similarity with RPA1, the largest subunit of the RPA heterotrimeric complex. Teb1 structure prediction revealed four OB folds, and at least two are responsible for sequence-specific telomeric ssDNA binding, and one is needed for interaction with TASC. Interestingly, the molecular weights of TASC components (75, 45, 19 kDa) mirror the sizes of RPA complex components, and p45 is predicted to contain one OB fold. Although Teb1 is similar to RPA1, it remains to be seen if TASC also forms an RPA-like structure. If it does, then Teb1 is an additional RPA1-like subunit that gets incorporated into an RPA-like complex. Teb1 interacts directly with telomeric ssDNA, and this interaction likely recruits the rest of the telomerase complex to telomeres *in vivo*.

In the light of the recent identification of RPA-like CST complexes in organisms other than *S. cerevisiae*, it is possible that *T. thermophila* may have evolved a CST complex (TASC and Teb1) that is telomerase-associated. Like yeast Cdc13, Teb1 binds sequence-specifically to telomeric ssDNA. Unlike ssDNA TBP, Teb1 does not act in telomere capping. Like the CST complex, Teb1 may coordinate telomere replication: vast overexpression of Teb1 causes division arrest and rapid loss of telomeres and subtelomeric regions from the rDNA chromosomes (BM and KC, unpublished data). In *S. pombe*, replication fork stalling and collapse at telomeres results in rapid loss of telomeres and subtelomeric regions in taz1 (dsDNA TBP) and trt1 (TERT) double mutant and in taz1 and RPA1 double mutant (Kibe et al., 2007; Miller et al., 2006). Like the CST

complex, Teb1 and TASC may function in telomere replication, in addition to their roles as telomerase proteins.

An interesting question is why telomerase evolved a TASC-mediated bridge to the telomere-binding Teb1 subunit. TASC may offer additional regulatory steps to control telomerase recruitment to telomeres. My investigation of the *T. thermophila* telomerase holoenzyme led to a successful holoenzyme reconstitution and uncovered a mechanism for how telomerase may be recruited to telomeres. *T. thermophila* telomerase may have evolved to constitutively associate with a CST-like complex, in order to couple telomerase activity and telomere replication, while keeping the POT1 complex at telomeres for capping functions. It will be interesting to study whether telomerase recruitment to telomeres and telomerase-mediated telomere elongation are separate from or dependent on other events in telomere replication.

CHAPTER TWO

An RPA-related Sequence-specific DNA Binding Subunit of Telomerase Holoenzyme is Required for Elongation Processivity and Telomere Maintenance

Abstract

Telomerase ribonucleoprotein complexes copy an internal RNA template to synthesize DNA repeats. DNA-interacting subunits other than telomerase reverse transcriptase (TERT) and telomerase RNA (TER) have been hypothesized to account for high repeat addition processivity of telomerase holoenzyme compared to the minimal catalytic RNP. Here we present the identification of three new subunits of *Tetrahymena thermophila* telomerase holoenzyme. Each of seven telomerase proteins is required for telomere maintenance and copurifies active RNP. The catalytic core (p65-TER-TERT) is assembled with a three-protein subcomplex (p75-p45-p19) and two peripheral subunits (p82 and p50). Remarkably, only a p82-enriched subset of the total holoenzyme population is capable of high repeat addition processivity, as shown by p82 immunodepletion and add-back. The RPA-like p82 subunit binds sequence-specifically to multiple telomeric repeats. These discoveries establish the existence of a telomerase holoenzyme processivity subunit with sequence-specific DNA binding.

Introduction

Telomeric repeats nucleate the formation of specialized chromatin that allows chromosome ends to persist as DNA breaks (Gilson and Geli, 2007b; Lue, 2009; Palm and de Lange, 2008). Each terminal repeat array is maintained in a dynamic equilibrium of repeat loss and new repeat synthesis. Telomerase elongates the guanosine-rich (G-rich) strand of telomeric repeats, T_2AG_3 in vertebrates or T_2G_4 in the ciliate *Tetrahymena thermophila,* using an active site within telomerase reverse transcriptase (TERT) and a template within telomerase RNA (TER). TERT and TER from some species can be combined in a heterologous cell extract to reconstitute telomeric repeat synthesis activity (Collins, 2009). Telomerase biogenesis and function in vivo require additional proteins that remain associated with TERT and TER in a telomerase holoenzyme (Collins, 2008; Gallardo and Chartrand, 2008). The catalytic features of recombinant TERT+TER can differ from the features of holoenzyme (Errington et al., 2008; Hardy et al., 2001). For example, for the relatively well-studied *T. thermophila* enzymes, the recombinant telomerase catalytic core differs from endogenous holoenzyme in the mechanism and extent of repeat addition processivity (RAP).

The current inventory of telomerase-associated factors includes proteins that interact with TER, TERT, and/or catalytically active holoenzyme. Among these factors, two types of holoenzyme protein have been most amenable to functional characterization. The first class is comprised of TER-binding proteins that promote accumulation of biologically stable, mature RNP (Teixeira and Gilson, 2007). These proteins are relatively straightforward to define by interaction assays and the in vivo depletion

phenotype of reduced TER. Ciliates possess a telomerase-specific protein with a La motif that folds and protects RNA Pol III-transcribed TER. RNA Pol II-transcribed TERs of vertebrates or yeasts instead assemble with proteins shared by small nuclear or small nucleolar RNPs. A second class of holoenzyme protein acts to allow telomerase engagement with the substrate single-stranded DNA (ssDNA) at chromosome termini (Gilson and Geli, 2007b). The best-characterized members of this group are budding yeast Est1 and Est3, which act in a coordinated, cell cycle-dependent fashion to activate the RNP catalytic core through a mechanism involving Est1 association with the telomeric ssDNA-binding protein Cdc13 (Chan et al., 2008; Osterhage et al., 2006; Pennock et al., 2001). Additional proteins in this category have been shown to affect telomerase subunit localization and association with telomeric chromatin (Fisher et al., 2004; Gallardo et al., 2008; Stellwagen et al., 2003; Venteicher et al., 2009).

Ciliates provide a favorable model system for telomerase holoenzyme characterization due to the relative abundance of active telomerase. We have focused on *T. thermophila* to exploit the useful combination of telomerase abundance and robust molecular genetic methods. Previous work discovered and characterized the *T. thermophila* telomerase holoenzyme proteins p65, p45, and p75 encoded by *TAP65*, *TAP45*, and *TAP75* (Witkin and Collins, 2004). In vivo depletion of the La motif-containing p65, but not p45 or p75, reduced the biological accumulation of TERT and TER. Biochemical and biophysical assays revealed that p65 binds and folds TER to promote subsequent TERT-TER interaction, producing a conformationally homogeneous p65-TER-TERT ternary complex (O'Connor and Collins, 2006; Prathapam et al., 2005; Stone et al., 2007). The in vitro assembly specificity of this RNP catalytic core parallels

that of TERT and TER accumulation as stable RNP in vivo. On the other hand, it remains unclear how p45 and p75 contribute to telomerase function. At a genetic level, these proteins have roles comparable to yeast Est1 and Est3, because protein depletion causes telomere shortening without loss of the RNP catalytic core (Lingner et al., 1997; Witkin and Collins, 2004). At a biochemical level, it has not been possible to assign activities or even protein-protein interaction specificities to p45 and p75, despite substantial effort.

To gain additional insight about telomerase holoenzyme proteins and their roles beyond assembly of the catalytic core, we sought to identify additional *T. thermophila* telomerase-associated proteins. Previous identification of p65, p45, and p75 involved large-scale purification of TERT-TAP (TERT tagged with a C-terminal calmodulin-binding peptide and tandem Protein A domains) overexpressed from an ectopically integrated transgene (Witkin and Collins, 2004). Although steady-state TERT accumulation was not increased in cells overexpressing TERT-TAP, continuous degradation of overexpressed protein led to identification of a TERT-associated but not holoenzyme-associated p20 protein, the Skp1 subunit of an abundant ubiquitin ligase. Genetic depletion of Skp1 increased rather than decreased telomere length, suggesting that this protein has a role in turnover of factor(s) that promote telomere elongation (Witkin et al., 2007). Here we exploit an improved affinity purification strategy and recent *T. thermophila* macronuclear genome annotation to discover three additional telomerase holoenzyme proteins designated p19, p50, and p82. The p19 subunit is part of a three-subunit 'telomere adaptor' subcomplex (p75-p45-p19). The DNA-binding p82 subunit joins the p75-p45-p19 subcomplex to confer the high repeat addition processivity of endogenous holoenzyme, while the substoichiometric p50 subunit modulates

association of the p75-p45-p19 subcomplex with the catalytic core. Overall this work reveals an intricacy of holoenzyme protein interactions that bridge the telomerase active site with a subunit capable of sequence-specific binding to telomeric ssDNA.

Results

Affinity Purification and Mass Spectrometry Identify Additional Telomerase Proteins

Based on previous studies, we designed a new strain for telomerase holoenzyme affinity purification. To avoid tagged TERT overexpression, we integrated a C-terminal tag cassette at the endogenous *TERT* locus such that tagged protein accumulation was dependent on expression from the endogenous promoter and translation from the endogenous open reading frame. In addition, we replaced the calmodulin-binding peptide of the previous TAP tag with 3xFLAG peptide, because the calmodulin-binding peptide reduces fusion protein expression level in *T. thermophila* and does not have high purification yield (Witkin et al., 2007). The new FZZ expression cassette (3xFLAG epitope/ Tobacco Etch Virus (TEV) protease cleavage site/ tandem Protein A domains) was integrated at *TERT* by selection for a linked neomycin resistance cassette (Figure 1A). Complete replacement of recombinant for endogenous chromosomes was obtained (Figure 1B), indicating that tagged TERT retains biological function.

Tandem steps of affinity purification were performed from whole-cell extract using two resins. The Protein A modules of the tagged protein were first bound to IgG agarose, followed by elution with TEV protease. The protease-cleaved fusion protein retained a 3xFLAG epitope and was next bound to FLAG antibody resin, followed by elution with 3xFLAG peptide or denaturant. To examine the protein profile of two-step purified samples, an aliquot of the FLAG antibody elution was subjected to SDS-PAGE and silver staining. Affinity purification of TERTfzz copurified several polypeptides not recovered in the parallel mock purification from extract without tagged protein (Figure

1C). Proteins with the mobilities of p75, p65, and p45 were readily detectable. In addition, we observed a yellow-orange band around 50 kDa that results from silver staining of TER. Additional polypeptides were also evident, only some of which could be assigned by immunoblotting to be degradation products of known holoenzyme proteins (for example, the indicated doublet of TERT N-terminal truncation products at ~100-110 kDa in Figure 1C).

The polypeptides specifically and reproducibly coenriched with TERT were identified by mass spectrometry comparison of TERTfzz and mock affinity purifications. To be comprehensive, the entire mixture of TERT-associated proteins eluted by denaturation was used for peptide sequencing, as described previously for human telomerase (Fu and Collins, 2007). *T. thermophila* gene identification was performed by searching the predicted proteome of the macronuclear genome (Coyne and al., 2008; Eisen and al., 2006). In addition to the known telomerase holoenzyme proteins TERT, p75, p65, and p45, the complete list of polypeptides specifically enriched with TERTfzz (Figure 1D) includes three proteins annotated as hypothetical in the *Tetrahymena* Genome Database. Each of the TERT-associated proteins was identified by at least two unique peptides (Figure 1D). Beyond these peptides, the open reading frames of the newly identified hypothetical proteins could have been incorrectly predicted by automated genome annotation. Therefore, mRNAs encoding these proteins were amplified by RT-PCR, cloned, and sequenced. The cloned cDNAs encoded proteins with predicted molecular weights of 19, 50, and 82 kDa (Figure 1D). In accordance with nomenclature rules, the genes were designated *TAP19*, *TAP50*, and *TAP82* for

Telomerase- or TERT-Associated Proteins; the proteins are described as p19, p50, and p82.

The newly identified p19 and p50 do not share obvious homology with any non-ciliate protein. In contrast, the domain architecture and primary sequence of p82 suggest that is has an evolutionary relationship with the Replication Protein A (RPA) largest subunit, RPA1. Domain structure modeling of p82 compiled by 3D-Jury suggests tandem OB folds most similar to those in human RPA1 (Supplemental Figure 1A). RPA1 proteins are top BLAST hits of p82 as well, with homology extending over the three RPA1 OB-fold DNA-binding domains (Supplemental Figure 1B). However, reciprocal BLAST of the *T. thermophila* genome with human RPA1 identifies a protein other than p82 as the top BLAST hit. The top BLAST hit is likely to be the actual *T. thermophila* ortholog of RPA1 based on sequence conservation and high expression level relative to p82. This putative *T. thermophila* RPA1 shares greater primary sequence identity with human RPA1 than either RPA1 shares with p82 (Supplemental Figure 1C), indicating that *TAP82* has substantially diverged from the putative ancestral *RPA1* (as also supported by biochemical data described below).

The predicted SDS-PAGE mobilities of the three newly identified proteins match polypeptides detected by silver staining, although at low silver-staining intensity (Figure 1C). In addition to the full-length proteins, small polypeptides are enriched that are likely degradation products of larger subunits (for example the 27 kDa polypeptide described below). The p19 polypeptide is likely the same protein observed in TERT-TAP purifications (Witkin and Collins, 2004) that appeared stoichiometric with TERT, p75, p65, and p45. On the other hand, p50 and p82 appear substoichiometric in their

holoenzyme association. Their identification suggests that we have deeply surveyed holoenzyme protein composition. However, because protein detection by mass spectrometry is not quantitative with regard to protein abundance, it remains possible that additional holoenzyme subunits remain to be discovered.

Newly Identified Proteins Have Essential Functions in Telomere Maintenance

To compare the biological function(s) of the newly identified proteins with known telomerase holoenzyme proteins, we first examined whether *TAP19*, *TAP50*, and *TAP82* are essential genes. For this purpose, we targeted each locus for replacement with a neomycin resistance cassette (Figure 2A). Because the expressed macronuclear genome is polyploid, initial transformants will be drug resistant but retain copies of the wild-type chromosome as well. Chromosome segregation is amitotic, resulting in some daughter cells with an increased ratio of recombinant to wild-type chromosome. If the targeted gene is not essential for growth, continued selective pressure yields cells with only the recombinant chromosome. If the gene is essential, cells will retain a mixture of wild-type and recombinant chromosomes. In multiple independent selections, endogenous wild-type *TAP19*, *TAP50*, or *TAP82* chromosomes could not be fully replaced (Figure 2A). Thus, like the previously characterized *T. thermophila* telomerase holoenzyme components, p19, p50, and p82 are essential.

Cells depleted for p19, p50, or p82 by gene knockdown were examined for a telomere length phenotype. Limiting the dose of TER, TERT, or any other holoenzyme subunit reduces the length of macronuclear telomeric repeats from the usual ~300 bp (Miller and Collins, 2000; Witkin and Collins, 2004; Witkin et al., 2007). Half of the *T.*

thermophila macronuclear telomeres share the same subtelomeric sequence, due to the amplification of a palindromic chromosome encoding the large rRNA precursor (the rDNA). If genomic DNA is digested with a specific restriction enzyme, denatured, resolved by PAGE, and hybridized with a subtelomeric-sequence oligonucleotide probe complementary to the G-rich or C-rich repeat strand, it is possible to detect change in length of both strands independently (Figure 2B). The denatured DNA strands resolve into a ladder that reflects the presence of a preferred telomeric-repeat permutation at chromosome 3' and 5' termini (Jacob et al., 2001). As observed previously in telomerase holoenzyme component knockdown strains, knockdown strains of p19, p50, and p82 had shorter G-strand and C-strand telomere lengths without loss of a preferential end-permutation (Figure 2B). This telomere shortening phenotype differs from the telomere elongation phenotype observed upon shut-off of the major *T. thermophila* ssDNA end-binding protein, Pot1a (Jacob et al., 2007). Because p19, p50, and p82 knockdown strains retain normal TER accumulation relative to a small nuclear RNA loading control (Figure 2C), as do p45 and p75 knockdown strains (Witkin and Collins, 2004; Witkin et al., 2007), these proteins influence a telomere maintenance step subsequent to stable assembly of the telomerase catalytic core.

Physical Associations Suggest an Overall Holoenzyme Subunit Architecture

To reciprocally confirm the association of the newly identified proteins with telomerase and to compare the physical interaction partners of all telomerase holoenzyme proteins in parallel, we took advantage of the two-step affinity purification developed for TERTfzz. Although mass spectrometry yields of a relative scarce enzyme such as

telomerase require many liters of culture input, approximately one liter of culture input is sufficient to detect TERTfzz-copurified proteins by SDS-PAGE and optimized silver staining. All proteins from the comprehensive list identified in association with TERTfzz (Figure 1D) were individually tagged at their endogenous locus using the C-terminal FZZ cassette. C-terminal TAP tagging of p65 and p45 was previously shown to produce biologically functional protein (Witkin and Collins, 2004). For these two subunits and the others discussed above (p75, p19, p50, and p82), C-terminal FZZ-cassette tagging also produced biologically functional protein, as demonstrated by complete substitution of recombinant for endogenous chromosomes (Supplemental Figures 2A and 2B; additional data not shown). Telomeres remained near wild-type length in cells expressing 65fzz, 45fzz, or 50fzz and were only slightly shorter than wild-type length in cells expressing 75fzz or 82fzz (Supplemental Figure 2C; additional data not shown). Telomeres had stable but notably shortened length in cells expressing 19fzz (Supplemental Figure 2C), suggesting that tagging this small protein partially compromised its biological stability or function.

Affinity purifications of each tagged protein were carried out under parallel conditions to compare the profile of copurified proteins. After two-step affinity purification, each tagged subunit migrates with an approximately 3 kDa difference from its endogenous counterpart due to the 3xFLAG tag fusion (Figure 3A, tagged subunits are indicated with open arrowheads). TERTfzz, 65fzz, 45fzz, 75fzz, 19fzz, and 82fzz copurified polypeptides with the migration of TERT and other holoenzyme proteins (Figure 3A; see Supplemental Figure 3A for immunoblots) as well as TER and telomerase activity (see below), reciprocally confirming their association. Compared to

the other purifications, tagged subunit yields from 19fzz or 82fzz purification were reproducibly lower. The low yield of 19fzz holoenzyme is likely a technical artifact of protein tagging, judging from the reduced telomere length of the 19fzz strain (described above) and the higher level of untagged p19 copurified with TERTfzz, 65fzz, and 45fzz (Figure 3A, compare lane 6 to lanes 2-4). The low yield of 82fzz holoenzyme instead appears to derive from ongoing subunit degradation and/or dissociation in extract: single-step affinity purifications recovered a level of holoenzyme comparable to TERTfzz (see below), but more extensive purification disproportionally reduced tagged p82 recovery. A scaled-up two-step affinity purification of 82fzz allowed holoenzyme copurification to be detected against high non-specific background (Figure 3A, lanes 7-9). In contrast, even scaled-up 50fzz purifications failed to enrich a protein detectable against the non-specific background, likely due to the extremely low expression level of p50 (50fzz was undetectable by immunoblot against the tag in whole-cell lysates; data not shown).

Across a range of extract preparation and purification conditions, the polypeptides that copurified with tagged holoenzyme subunits had the SDS-PAGE mobilities of other holoenzyme subunits, not of unknown proteins. These findings suggest that the *T. thermophila* telomerase proteins are likely telomerase-specific in assembly and function, unlike the telomerase-associated proteins of mammalian cells. Several additional observations emerged from the course of these purification assays. Addition of the proteasome inhibitor MG132 to extracts before purification improved the recovery p82 and p50 with other holoenzyme components (Figure 3B, compare lanes 3-4). In addition, we observed variable mobility of p65, including at least two forms enriched by the C-terminal tag (Figure 3B, lanes 5-6). Finally, small polypeptides not corresponding to full-

length holoenzyme proteins varied in their extent of copurification with the tagged subunits. A 27 kDa polypeptide showed decreased recovery in purifications with MG132 (Figure 3B, compare lanes 3 and 5 with lanes 4 and 6) and generally showed a reciprocal relationship with full-length p82, suggesting that it could be p82 proteolytic fragment. In addition, 30 and 26 kDa polypeptides were enriched preferentially by 65fzz (Figure 3B, compare lanes 5-6 with 3-4), which could reflect p65 proteolysis or the participation of additional proteins in an early stage of telomerase RNP assembly.

We exploited the relatively robust yield of TERTfzz, 65fzz, and 45fzz purifications to assay protein-protein interactions within the holoenzyme. Leaving the second-step FLAG-tagged complexes immobilized on antibody resin, we performed an incubation with RNase A or buffer control, washed to remove dissociated subunits, and eluted with FLAG peptide prior to SDS-PAGE and silver staining. RNase treatment of TERTfzz holoenzyme induced an apparent misfolding of TERT that affected protein recovery, likely by interfering with tag accessibility (Figure 4A, lanes 1-2). RNase treatment of p65fzz holoenzyme depleted all holoenzyme subunits except p65 (Figure 4A, lanes 3-4). RNase treatment of 45fzz holoenzyme depleted TERT and p65 while p45 and p75 remained associated with each other as an RNase-resistant subcomplex (Figure 4A, lanes 5-6; see Supplemental Figure 3B for p65, p45, and p75 immunoblots). This subcomplex also contained p19 (Figure 4A, lanes 5-6; see Supplemental Figure 3B for p19 immunoblot). This physical interaction of p75, p45, and p19 subunits is consistent with their shared in vivo depletion phenotype of telomere shortening without loss of TER RNP.

To bypass the limitation of low endogenous p82 or p50 recovery with two-step purified holoenzyme, we attempted to bacterially express and purify recombinant p82 and p50 for holoenzyme supplementation in vitro. This was successful only for recombinant p82 (r82), which could be purified as a soluble 6xHis-tagged protein (see below). After supplementing purified 65fzz or 45fzz holoenzyme with r82 and washing to remove excess protein, we examined the RNase-sensitivity of protein-protein interactions. Some non-specific association of r82 with antibody resin was detected in the absence of RNase A (Figure 4B, lanes 1-2). RNase treatment of r82-supplemented 65fzz holoenzyme released all proteins other than p65 itself, with only background levels of r82 association (Figure 4B, lanes 3-4). On the other hand, RNase treatment of r82-supplemented 45fzz holoenzyme reproducibly retained an elevated level of r82 in association with the p75-p45-p19 subcomplex (Figure 4B, lanes 5-6). These results suggest that the p75-p45-p19 subcomplex recruits p82 through protein-protein interactions. Overall, the findings described above suggest that a biologically stable assembly of the RNP catalytic core (p65-TER-TERT) associates directly with a second holoenzyme protein subcomplex (p75-p45-p19) that is required as an adaptor for p82 binding and telomerase function at telomeres in vivo (Figure 4C).

Holoenzyme Proteins Differentially Enrich High Repeat Addition Processivity

Tagged TERT, TER, p75, p65, and p45 copurify telomerase catalytic activity from cell extracts (Cunningham and Collins, 2005; Witkin and Collins, 2004; Witkin et al., 2007). Using the panel of FZZ strains created above, we compared the ability of known and newly identified proteins to associate with telomerase catalytic activity.

Complexes recovered from extract by single-step binding to FLAG antibody resin were divided for parallel analysis of TER (Figure 5A, top panel) and telomerase activity (Figure 5A, main panel). Activity was assayed by direct primer extension of the telomeric repeat oligonucleotide $(GT_2G_3)_3$ in reactions with dTTP and radiolabeled dGTP. All of the tagged proteins copurified telomerase activity, with amounts of activity proportional to the relative enrichment of TER (Figure 5A).

Telomerase holoenzyme purified by TERTfzz, 65fzz, 45fzz, 75fzz, 19fzz, or 50fzz catalyzed the synthesis of a similar product profile, with an accumulation of both short and long products (Figure 5A). In distinction, telomerase holoenzyme purified by 82fzz catalyzed predominantly long-product synthesis (Figure 5A, lane 7). This selective enrichment of high-RAP activity was also observed with two-step affinity purification of 82fzz (Figure 5B). To confirm this TERTfzz versus 82fzz enzyme population difference, we performed a reaction time-course (Supplemental Figure 4). The TERTfzz-enriched holoenzyme population had high-RAP activity, generating products that gained length over time, and also had low-RAP activity, producing short products that increased in abundance but not length due to enzyme turnover. The 82fzz-enriched holoenzyme had high-RAP activity but much less low-RAP product synthesis; a small amount of low-RAP activity could derive from p82 dissociation from holoenzyme in the activity assay reaction.

To confirm that untagged p82 is also preferentially associated with high-RAP activity, we used TERTfzz-purified holoenzyme for an immunoenrichment assay with preimmune or p82 antiserum (Figure 5C). Incubation with p82 antibody but not preimmune serum depleted high-RAP activity, while low-RAP activity remained in the

unbound fraction (Figure 5C, lanes 1-3). The p82 antibody selectively retained high-RAP activity (Figure 5C, lanes 4-5), similar to the enrichment observed by affinity purification of 82fzz (Figures 5A and 5B). These experiments reveal that the telomerase holoenzyme population assayed in cell extract includes at least two catalytically distinct forms, differentiated in subunit composition by the presence or absence of p82 (Figure 4C). This finding provides a rationale for the variability in RAP observed across *T. thermophila* extracts or fractionations: conditions that allow proteolysis diminish the recovery of high-RAP activity (Supplemental Figure 5A).

Recombinant p82 Stimulates RAP and Binds Telomeric ssDNA

Among the seven tagged holoenzyme proteins that individually copurified active telomerase, only 82fzz did not enrich low-RAP activity (Figure 5A). This observation and the immunodepletion of high-RAP but not low-RAP activity with p82 antibody (Figure 5C) suggested that p82 could directly affect holoenzyme RAP. We therefore tested whether a TERTfzz-purified holoenzyme population with predominant low-RAP activity could be rescued to high RAP by addition of p82 alone. We added bacterially expressed and purified r82 (Figure 6A) or buffer control to two-step purified TERTfzz holoenzyme or a mock affinity purification immobilized on FLAG antibody resin, washed, and eluted with FLAG peptide. Holoenzyme incorporation of r82 (Figure 6B) induced a loss of low-RAP activity and a gain of high-RAP activity (Figure 6C). Similar results were observed if r82 was added directly to the activity assay itself (Supplemental Figure 5B). On the other hand, r82 addition to the *T. thermophila* telomerase catalytic

core reconstituted in RRL did not stimulate RAP (data not shown), consistent with holoenzyme association of p82 via the p75-p45-p19 subcomplex (Figure 4B).

The high-RAP products of *T. thermophila* telomerase holoenzyme continue to elongate over an extended reaction time course (Cunningham and Collins, 2005). Using an initial pulse of radiolabeled dGTP and a chase of unlabeled dGTP, the longest products do not reach a steady-state distribution, but products with short and intermediate lengths can be resolved that are resistant to chase and thus can be used as elongation end-points for a RAP calculation (Figure 6D). Quantification of the chased low-RAP products (Figure 6D, lane 2; bracketed Low RAP products) normalized for dGTP incorporation revealed that the efficiency of next-repeat synthesis approaches only 30%, similar to the maximal efficiency obtained by *T. thermophila* TERT+TER reconstituted in RRL (Hardy et al., 2001). Addition of r82 eliminated the synthesis of low RAP products, shifting the holoenzyme population to intermediate and high RAP product synthesis (Figure 6D, compares lanes 1-2 with lanes 3-4). Minimal estimates of RAP, based on the chased intermediate-length products (Figure 6D, lanes 2 and 4; bracketed Intermediate RAP products), indicate a 50-80% efficiency of next-repeat synthesis, much greater than that supported by the TERT+TER RNP alone.

One obvious mechanism by which p82 could act as a processivity factor would be to contact ssDNA, thereby stabilizing holoenzyme association with its product. Sequence analysis of p82 predicted the presence of tandem OB folds similar to the three OB-fold DNA-binding domains of RPA1 (Supplemental Figure 1). RPA1 provides the primary contact surface for DNA within the RPA heterotrimer, which recognizes an extended 20-30 nt length of ssDNA largely independent of sequence (Bochkarev and Bochkareva,

2004; Iftode et al., 1999; Wold, 1997). We therefore assayed the DNA binding activity of r82 by electrophoretic mobility shift assay using 5'-fluorescein-labeled (6FAM) oligonucleotides with either non-telomeric sequence, three G-rich telomeric repeats, three C-rich telomeric repeats, or the G-rich and C-rich repeats annealed to form a duplex (Supplemental Table 1). Remarkably, despite its similarity to RPA1, r82 shifted only the G-rich telomeric-repeat ssDNA (Figure 6E). The non-telomeric and C-rich telomeric-repeat ssDNAs and the telomeric-repeat duplex were not recognized by p82. Thus, although p82 shows biochemical similarity to RPA1 in its ability to bind ssDNA, it differs from RPA1 in the requirement for a specific ssDNA sequence. This distinction in DNA interaction specificity is consistent with the sequence divergence of p82 from both *T. thermophila* and human RPA1 (Supplemental Figure 1C).

Binding of r82 to the 6FAM-labeled three-repeat G-rich telomeric strand was competed by addition of unlabeled three-repeat but not two-repeat G-rich telomeric DNA (Figure 6F, lanes 1-8). Four-repeat ssDNA forms folded structures under assay conditions, but extending the three-repeat sequence with six additional non-telomeric 3' or 5' nucleotides increased competition activity (Figure 6F, lanes 9-14), suggesting that r82 binds better to the longer ssDNAs. In addition, these results suggest that p82 does not specifically recognize a telomeric repeat at the ssDNA 3' terminus, unlike the telomere end-binding protein complex from *Oxytricha nova* (Horvath et al., 1998). Competition was ineffective if the telomeric-repeat guanosines were substituted by other purines, or if human telomeric repeats or scrambled *T. thermophila* telomeric repeats were used (Figure 6F, lanes 15-26). Some of these modified sequences showed limited competition at much higher concentration (Supplemental Figure 6). We used 5'-radiolabeled rather

than 6FAM-labeled versions of the optimal competitor oligonucleotides to calculate r82 binding affinities for TeloG3-NT6 and NT6-TeloG3, which were 80 and 200 pM, respectively (Figure 6G).

Overexpression of p82 or p50 Alters Holoenzyme Composition and Telomere Maintenance

The substoichiometry of p50 and p82 in TERTfzz-purified telomerase holoenzyme suggested that cells could regulate telomerase function by limiting the expression of peripheral holoenzyme subunits. To investigate whether increasing the level of p50 or p82 expression would affect their association with holoenzyme and/or telomerase function at telomeres, we introduced transgenes directing cadmium-inducible expression of untagged p50 or p82 into the TERTfzz strain background (Figure 7A). The *MTT1* promoter used for cadmium-inducible protein overexpression to high cellular level (Shang et al., 2002) also has a basal level of transcription that represents modest mRNA overexpression for scarce telomerase subunits (Lee and Collins, 2007; Miao et al., 2009).

Curiously, even vast overexpression of p50 with cadmium induction did not increase p50 association with TERTfzz-purified holoenzyme (Figure 7B). Instead, although TERTfzz still copurified p65, association of the RNP catalytic core with p75, p45, p19, and p82 was reduced (Figure 7B, compare lanes 2 and 4). As might be expected from this change in holoenzyme composition, p50 overexpression also induced telomere shortening (Figure 7C). Cadmium-induced overexpression of p82 increased its copurification with TERTfzz holoenzyme and also enhanced the copurification of smaller polypeptides that may be p82 degradation products (Figure 7B, compare lanes 2 and 3).

Vast p82 overexpression caused rapid cell cycle arrest (data not shown), while modest overexpression of p82 without cadmium allowed culture growth but induced telomere shortening (Figure 7C). These experiments suggest that the expression level of the holoenzyme subunits p50 and p82 must be regulated to achieve normal telomere length homeostasis.

Discussion

New Telomerase Proteins Add Subunits and Subcomplexes to Holoenzyme Architecture

The aim of this work was to identify and biologically characterize all subunits of a telomerase holoenzyme, enabled by the use of *T. thermophila* as a model system. By fusing an optimized affinity purification tag to the C-terminus of TERT at its endogenous locus, we were able to coenrich known and unknown telomerase holoenzyme proteins. The first insights about telomerase holoenzyme architecture that emerge from characterization of an eight-factor set of components include several surprises. At a first level, it is striking that telomerase holoenzymes from a single-celled eukaryote harbor so many subunits, each of which is required for telomere maintenance. Also, in *T. thermophila,* all of the subunits appear telomerase-specific in their associations rather than shared among multiple classes of nuclear RNP. Furthermore, six *T. thermophila* telomerase holoenzyme subunits are approximately stoichiometric when purified from asynchronously dividing cells (TER, TERT, p65, p75, p45, p19), but at least one subunit appears biologically substoichiometric in association and function (p50). The p82 subunit is also under-represented in purified holoenzyme. The *Saccharomyces cerevisiae* telomerase proteins Est1 and Est3 may be substoichiometric with other holoenyzme components as well, because they are depleted from the catalytic core in G1 phase of the cell cycle (Osterhage et al., 2006). Thus, even in organisms with constitutive telomere maintenance and relatively many telomeres per genome content of DNA, telomerase regulation gives rise to holoenzyme complexes with differential subunit composition.

Subunit interaction studies uncovered the presence of holoenzyme subcomplexes. Previous genetic and biochemical assays demonstrate codependent assembly of p65, TER, and TERT to form a stable catalytic core (O'Connor and Collins, 2006; Prathapam et al., 2005; Stone et al., 2007; Witkin and Collins, 2004). Studies of the expanded inventory of TERTfzz-copurified proteins revealed another holoenzyme subcomplex, the p75-p45-p19 telomere adaptor complex, built by protein interactions among subunits required for telomere maintenance but dispensable for formation of the RNP catalytic core. Two additional subunits, p82 and p50, join the holoenzyme in a manner that is peripheral to the stability of RNP catalytic core or telomere-adaptor subcomplex. The extremely low endogenous expression level of p50 and the refractory behavior of recombinant protein expressed in *E. coli* limited the scope of biochemical analysis. However, we note that the profile of telomerase product synthesis associated with 50fzz (Figure 5A) indicates that this subunit associates with both low-RAP and high-RAP activity. Thus, p50 can join holoenzyme complexes with or without functional p82.

Sequence-specific ssDNA Binding by a Telomerase Holoenzyme Protein Processivity Factor

Sequence analysis of p82 suggests that its structural similarity with RPA1 encompasses the RPA1 DNA binding domains. Indeed, although their specificity for sequence differs, p82 and RPA1 share a binding preference for a relatively extended, ~20-nt length of ssDNA (Bochkarev and Bochkareva, 2004; Iftode et al., 1999; Wold, 1997). The 3-4 telomeric-repeat length of ssDNA required for recognition by p82 is much longer than the ssDNA length required for sequence-specific binding by telomere

proteins, which are sensitized to recognition of a few critical residues within 1-2 repeats (Croy and Wuttke, 2006). Considering the different biological roles of p82 and a telomere protein, this fundamental difference in recognition specificity makes sense. Telomerase holoenzyme should engage its substrate during genome replication, when long tracts of G-rich ssDNA are exposed, but not during interphase, when only shorter tracts of G-rich repeats are accessible. Also, considering p82 function within a telomerase holoenyzme, recognition of a long surface of ssDNA by p82 could allow dynamic individual contacts while maintaining stable protein-DNA association overall.

The telomerase holoenzyme context of p82 function obliges a major distinction from RPA1 in protein interaction specificity: instead of the RPA heterotrimer, p82 associates with the telomere adaptor subcomplex of telomerase holoenzyme. How the specificity of p82 interaction with p75, p45, and/or p19 is achieved remains to be explored, after the development of a reconstitution system for the telomere adaptor subcomplex. In *S. cerevisiae*, the telomeric-repeat binding protein Cdc13 alternates between a partnership with telomerase holoenzyme, which stimulates telomere elongation, or a partnership with Stn1 and Ten1, which provides telomere end-protective function (Li et al., 2009; Pennock et al., 2001). An RPA-like architecture of complex formation has been proposed to underlie interactions in the Cdc13-Stn1-Ten1 complex (Gao et al., 2007). It is possible that p75, p45, and/or p19 provide an interface for RPA-like multimerization with p82. It is also possible that p82 contacts telomere proteins, potentially in transient fashion. Approaches other than affinity purification under native conditions will be necessary for exploring the full scope of p82 interactions in vivo.

Endogenous p82 differentiates the purified holoenzyme population with high-RAP activity from the population with low-RAP activity, and supplementation of a mixed holoenzyme population with recombinant p82 converted the low-RAP enzyme to higher RAP. Like p82, the telomeric-repeat ssDNA-binding complex POT1-TPP1 can stimulate human telomerase RAP in vitro, but unlike p82, association between these telomere proteins and telomerase holoenzyme is transient and potentially indirect (Wang et al., 2007; Xin et al., 2007). The existence of a holoenzyme subunit beyond the RNP catalytic core with independent DNA binding activity provides a mechanism to improve RAP but presents also an interesting challenge for telomerase negotiation with its product: as each newly synthesized repeat is displaced from the active site, does new product associate with p82 or does p82 remain bound to the initial site of interaction? These alternatives have biological implications in the coordination of telomere maintenance and will be fascinating to explore as a novel mechanism of processivity. The extremely high RAP that p82-bound holoenzyme can accomplish in vitro over an extended time course is unlikely to occur in the context of a replicating telomere in vivo (Yu and Blackburn, 1991). Instead, high RAP may be the signature of telomerase holoenyzme ability to associate tightly with telomeric-repeat ssDNA. The insights about telomerase holoenyzme protein architecture and DNA binding specificity uncovered here will enable direct assays of how telomerase subunit interactions with the telomere are regulated and coordinated other with chromosome replication machineries.

Materials and Methods

Affinity Purification and Mass Spectrometry

Two-step purification was carried out by batch binding for 2-4 h at 4°C with 200 µl rabbit IgG-agarose (Sigma) for each 10 mL of extract representing 500 mL of initial cell culture. Subsequent steps were done at room temperature in T2EG50 (20 mM Tris-HCl pH 8.0, 1 mM EDTA, 10% glycerol, 50 mM NaCl, 5 mM β-mercaptoethanol or 5 mM DTT) supplemented with 0.1% Igepal CA-630. Washed IgG agarose was incubated with 30 µg/mL TEV protease for 0.5-1 h. Eluted samples were batch-bound to 10-15 µl of EZView Red anti-FLAG M2 resin (Sigma) in low-retention tubes for 1-2 h. Washed resin was incubated with 150 ng/µl of 3xFLAG peptide (Sigma) for 30-60 min. For mass spectrometry, samples were eluted from M2 resin with 100 mM glycine pH 2.5, neutralized with 2 M Tris base, precipitated with trichloracetic acid, then processed as described previously (Fu and Collins, 2007). Single-step purification was performed by batch-binding extract to 20 µl FLAG antibody resin for 2-4 h at 4°C.

Strain Construction

Gene knockout constructs targeted the entire coding region for replacement by neo2. FZZ tagging constructs included the endogenous coding region sequence, the FZZ tag, a stop codon, 3' UTR sequence including the polyadenylation signal of *RPL29*, and neo2. Transformation and paromomycin selection for strains with a neo2 cassette were performed as previously described (Miller and Collins, 2000). Transgenes for integration at *BTU1* replaced the *BTU1* promoter and open reading frame with the gene of interest

under expression control by ~1 kbp of the *MTT1* promoter (Shang et al., 2002). Transformation and paclitaxel selection for *BTU1* targeting in strain CU522 were performed as described (Witkin and Collins, 2004).

Extract Preparation

Cells were grown to mid-log phase ($3.5x10^5$ cells/mL) at 30°C in modified PPYS (1% proteose peptone, 0.2% yeast extract, 2% glucose, 50 μM $FeCl_3$) or modified Neff (0.25% proteose peptone, 0.25% yeast extract, 0.5% glucose, 30 μM $FeCl_3$). Harvested cells were washed with 10 mM Tris-HCl pH 7.5 and lysed with ice-cold 0.2% Nonidet P-40 substitute (Igepal CA-630) and 0.1% Triton X-100 in T2EG50 buffer with 1/1000 volume of Sigma protease inhibitor cocktail (AEBSF, aprotinin, bestatin, E-64, leupeptin, pepstatin A) and 0.1 mM PMSF. Except for the initial affinity purification used for mass spectrometry (Figure 1C), most purifications shown used 5 μM MG132 (Calbiochem) added to lysis buffer immediately prior to cell lysis. Lysis was allowed to proceed for 15 min at 4°C followed by centrifugation for 1 h at 4°C and 100,000-130,000 x *g* (S-100 extract) or 10,000 x *g* for 10 min (low-speed extract for rapid single-step purifications). Extract was used immediately or flash frozen in liquid nitrogen and stored at -80°C until use.

Nucleic Acid Purification and Hybridization

RNA was purified using TRIzol (Invitrogen) and resolved on 6% acrylamide/7 M urea gels before electrophoretic transfer to Hybond-N^+ (GE Heathcare). Blots were probed with end-labeled oligonucleotides. For genomic DNA purification, cells from 2 mL of

culture were washed with 10 mM Tris-HCl pH 7.5 and lysed with 0.7 mL urea buffer (10 mM Tris-HCl pH 7.5, 0.35 M NaCl, 10 mM EDTA, 1% SDS, 42% urea). Lysate was extracted twice with PCI (phenol:chloroform:isoamyl alcohol, 25:24:1) and once with chloroform:isoamyl alcohol (24:1), 150 µl of 5 M NaCl was added, and DNA was precipitated with isopropanol. DNA spooled into a new tube was washed with 75% ethanol, dried, and resuspended in TE (10 mM Tris pH 8.0, 1 mM EDTA), treated with RNase A, and digested with restriction enzymes of choice for integration tests or with HindIII for rDNA telomere analysis. Digested DNA was recovered by PCI extraction and ethanol precipitation, resolved using non-denaturing 0.8% agarose/1X TBE for integration tests or denaturing 6% acrylamide/7 M urea/0.6X TBE for telomere blots, transferred to Hybond-N^+ membrane, and probed. Random hexamer labeling was used to make probes for integration tests; rDNA subtelomeric-sequence oligonucleotides were end-labeled to make probes for telomere blots. Data was collected with a Typhoon Trio Imager. Markers for the telomere blots should be considered approximate, because the DNA marker (Invitrogen) and *T. thermophila* rDNA chromosome sequences are analyzed in denatured state and do not have balanced nucleotide content.

Subunit Association Assays

Telomerase holoenzyme bound to FLAG antibody resin was treated with 10 µg RNase A or mock-treated in 100 µl T2MG (20 mM Tris pH 8.0, 1 mM $MgCl_2$, 10% glycerol) with 50 mM NaCl (T2MG50) supplemented with 0.1% Igepal and 5 mM β-mercaptoethanol for 15 min at room temperature (RT). For assaying r82 interaction with holoenzyme proteins, 5 µg r82 in 100 µl T2MG50 was incubated with holoenzyme for 30 min at RT

prior to RNase treatment. For r82 reconstitution with intact holoenzyme, r82 and holoenzyme were incubated in blocking wash buffer (T2MG50, 0.1% Igepal, 5 mM DTT, 0.1 mg/ml heparin, 0.1 mg/ml casein) with or without 1 µg r82 in 100 µl volume for 30 min at RT. Activity was assayed in an aliquot of resin prior to elution, while proteins were examined by SDS-PAGE after elution with FLAG peptide.

Telomerase Activity Assays

Resin-bound samples were washed into T2MG supplemented with 5 mM β-mercaptoethanol. Activity assays reaction buffer had final concentrations of 50 mM Tris-acetate pH 8.0, 10 mM spermidine, 5 mM β-mercaptoethanol, 2 mM $MgCl_2$, 0.4 mM dTTP, 0.3 µM dGTP, 33 nM [α-^{32}P]dGTP (NEN/Perkin Elmer EasyTide 3000 Ci/mmol), and 50-100 nM $(GT_2G_3)_3$ primer. Reactions proceeded for 6-30 min at 30°C before quenching with TES (50 mM Tris-HCl pH 8.0, 20 mM EDTA, 0.2% SDS). For the chase experiment, reactions were incubated for 10 min as noted above before addition of dGTP to 30 µM final (100-fold excess over the radiolabeled pulse) for a chase of another 10 min at 30°C. In assays including r82, r82, telomerase, and primer were incubated together at RT for 10 min before the addition of buffer and nucleotides. Products were extracted with PCI and precipitated with carriers (10 µg yeast tRNA, 10 µg glycogen, 25 µg linear polyacrylamide) and 0.3 M ammonium acetate in ethanol. Pellets were washed once with 75% ethanol, dried briefly, and resuspended in 5 µl of formamide with 10 mM EDTA and tracking dyes. Products were boiled, snap-cooled, and resolved on 9-10% acrylamide/7 M urea denaturing gels. Images were collected with a Typhoon Trio Imager and quantified with ImageQuant software.

Recombinant Protein Purification and Gel Mobility Shift

A synthetic gene encoding r82 was subcloned into pET28 and transformed into BL21 (DE3). Protein expression was induced with 0.1 mM IPTG at 16°C. Cells were resuspended in T2MG with 250 mM NaCl and sonicated to lyse, then 0.1% Igepal and an additional 50 mM NaCl were added before clearing the lysate. Tagged protein was bound to Ni-NTA agarose (Qiagen) with 20 mM imidazole at 4°C for 3 h before washing and eluting the same binding buffer supplemented to 300 mM imidazole. Purified protein was adjusted to 5 mM DTT and flash frozen.

All oligonucleotides were gel-purified before use (IDT DNA; see Supplemental Table 1 for probe and competitor sequences). Probe concentration was ~10 nM for 6-carboxyfluorescein-labeled oligonucleotides or ~1 pM for radiolabeled oligonucleotides; protein and competitor concentrations are given in Figure legends. Final binding buffer contained 10 mM Tris-HCl pH 8.0, 0.5 mM $MgCl_2$, 5% glycerol, 150 mM NaCl, 150 mM imidazole, 0.05% Igepal, 0.5 µg/µl BSA, and 0.1 µg/µl tRNA. Binding was conducted for 10 min at RT. Order-of-addition experiments verified that interaction equilibrium was reached within the incubation time. Samples were resolved on a 5% acrylamide gel (37.5:1 acrylamide:bisacrylamide) with 4% glycerol and 0.5X TBE run at 4°C. Data was collected using a Typhoon Trio Scanner, and binding affinity was calculated using ImageQuant software based on free probe signal.

Antibodies

Full-length recombinant p19 or p82 was used to generate rabbit polyclonal antibody. Rabbit polyclonal antibodies against p65, p75, and p45 were generated previously using full-length proteins (Witkin et al., 2007).

Immunodepletion

Antibody resin was prepared with Protein A Sepharose 4 FastFlow (Amersham) and preimmune or p82-immununized serum: 20 µl of resin was incubated with 100 µl serum and 100 µl PBS for 1.5 h at RT, washed with PBS, washed with T2MG with IT (0.2% Igepal, and 0.1% Triton X-100) and 0.5 M NaCl, and washed into binding buffer (T2MG IT with 50 mM NaCl, 1/1000 volume of Sigma protease inhibitor cocktail, 0.5 mg/ml BSA). Holoenzyme purified on IgG resin and eluted with TEV protease was used for immunodepletion, with incubation at 4°C for 1 h before removing the unbound fraction and washing the resin twice in binding buffer at RT for 10 min.

GenBank Accession Numbers

Accession numbers are EU873082 for *TAP19*, EU873083 for *TAP50*, EU873081 for *TAP82*, and GQ274003 for *T. thermophila RPA1*.

Figure 1. Affinity Purification and Mass Spectrometry Identify Additional TERT-Associated Proteins

(A) Diagram of FZZ-tagging strategy at the *TERT* locus.

(B) FZZ cassette integration. Replacement of the wild-type (WT) *TERT* locus by the FZZ-tagged recombinant (neo2) locus was detected by Southern blot.

(C) Two-step affinity purification of TERTfzz and associated proteins.

(D) TERTfzz-associated proteins identified by mass spectrometry.

A

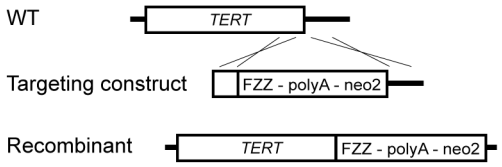

B

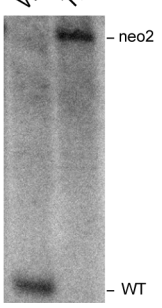

C

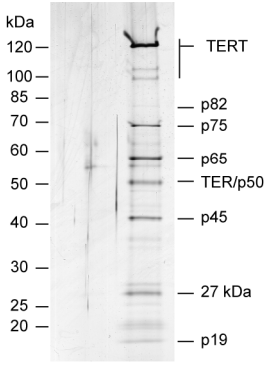

D

TTHERM ID	ORF	Unique peptides	Percent coverage	MW (kDa)	pI	Domains
00112560	TERT	16	19	133	9.3	
00218760	Hypothetical	5	10	82	8.2	OB folds
00059040	TAP75	15	27	74	7.8	
00318530	TAP65	5	12	64	6.9	La motif
01049190	Hypothetical	9	24	50	9.0	
00083360	TAP45	7	26	44	5.9	
00658760	Hypothetical	2	11	19	8.2	

Figure 2. Newly Identified Proteins are Essential for Telomere Maintenance

(A) Partial gene disruption for *TAP19*, *TAP50*, and *TAP82*. A diagram of the gene disruption strategy is shown.

(B) Telomere length in *TAP19*, *TAP50*, and *TAP82* knockdown cultures.

(C) Northern blot for accumulation of TER and U6 RNA.

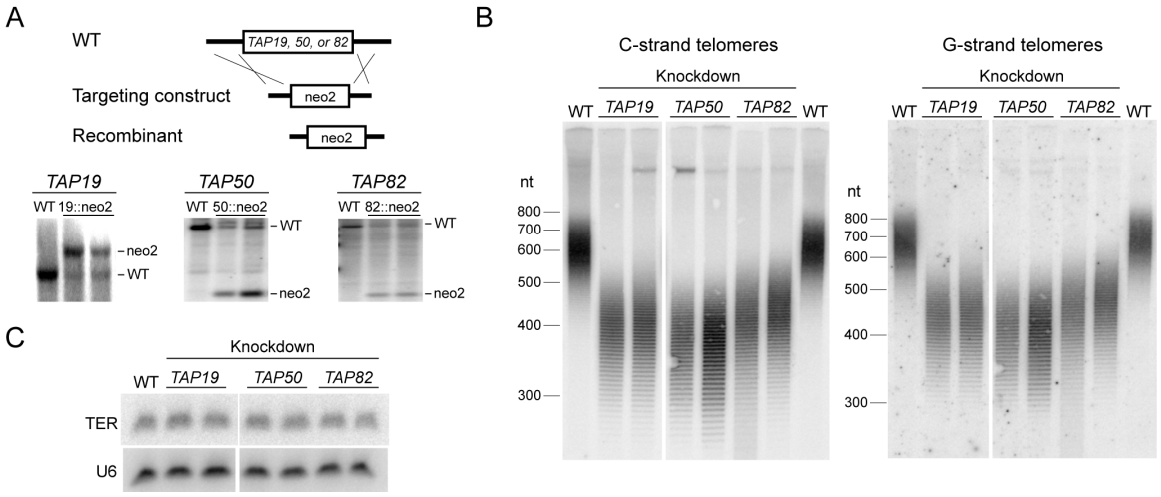
A
WT
TAP19, 50, or 82
Targeting construct
neo2
Recombinant
neo2
TAP19
WT 19::neo2
neo2
WT
TAP50
WT 50::neo2
WT
neo2
TAP82
WT 82::neo2
WT
neo2
B
C-strand telomeres
Knockdown
WT TAP19 TAP50 TAP82 WT
nt
800
700
600
500
400
300
G-strand telomeres
Knockdown
WT TAP19 TAP50 TAP82 WT
nt
800
700
600
500
400
300
C
Knockdown
WT TAP19 TAP50 TAP82
TER
U6

Figure 3. FZZ-tagged Proteins Purify Other Telomerase Holoenzyme Subunits

Two-step affinity purifications were performed to enrich fzz-tagged protein complexes. Open arrowheads indicate the tagged protein.

(A) Copurification of telomerase holoenzyme proteins. Purifications in lanes 7-9 used more input extract and thus have greater non-specific background.

(B) Effect of MG132 on purified holoenzyme subunit composition.

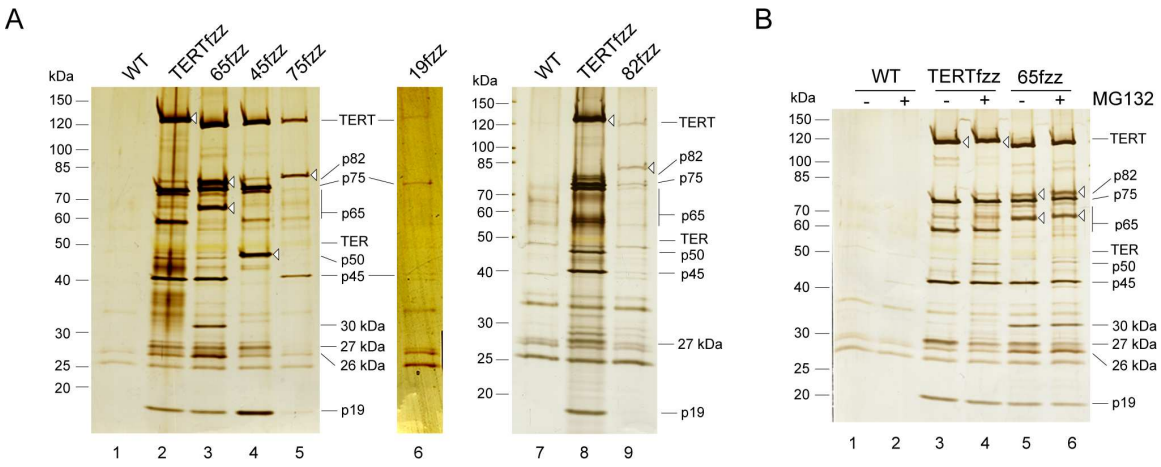
A
WT
TERTfzz
65fzz
45fzz
75fzz
19fzz
82fzz
kDa
150
120
100
85
70
60
50
40
30
25
20
TERT
p82
p75
p65
TER
p50
p45
30 kDa
27 kDa
26 kDa
p19
1
2
3
4
5
6
7
8
9
B
MG132
-
+
1
2
3
4
5
6

Figure 4. Protein Interactions Establish A Second Holoenzyme Subcomplex

(A) Identification of a p75-p45-p19 subcomplex. Immobilized holoenzyme complexes were treated with RNase A.

(B) Association of p82 with the p75-p45-p19 subcomplex. Recombinant p82 (r82) was added to immobilized holoenzyme followed by treatment with RNase A.

(C) Summary of telomerase subcomplexes.

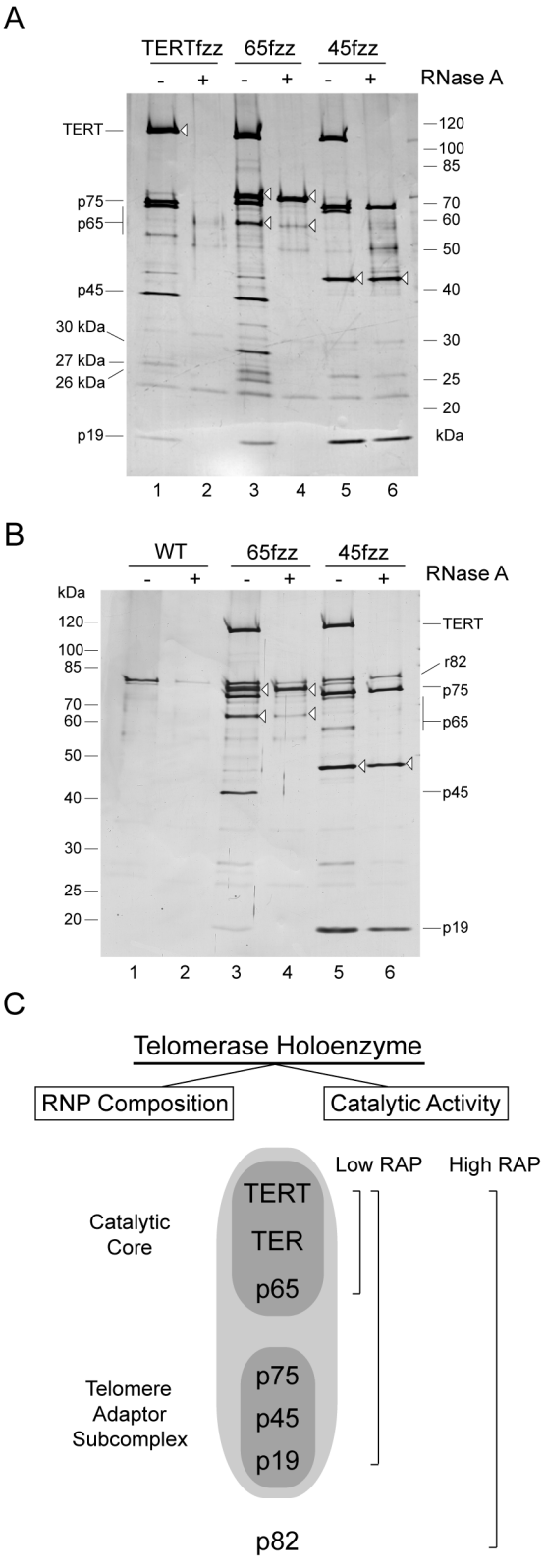
A
TERTfzz
65fzz
45fzz
- + - + - +
RNase A
TERT
p75
p65
p45
30 kDa
27 kDa
26 kDa
p19
120
100
85
70
60
50
40
30
25
20
kDa
1 2 3 4 5 6
B
WT
65fzz
45fzz
- + - + - +
RNase A
kDa
120
100
85
70
60
50
40
30
25
20
TERT
r82
p75
p65
p45
p19
1 2 3 4 5 6
C
Telomerase Holoenzyme
RNP Composition
Catalytic Activity
Low RAP
High RAP
Catalytic Core
TERT
TER
p65
Telomere Adaptor Subcomplex
p75
p45
p19
p82

Figure 5. Tagged Holoenzyme Proteins Copurify TER and Telomerase Activity

(A) TER and telomerase activity enriched by fzz-tagged proteins using single-step purification on FLAG antibody resin.

(B) High-RAP telomerase activity enriched by 82fzz. TERTfzz and 82fzz cell extracts were used for two-step affinity purification followed by activity assay. The same samples were analyzed by SDS-PAGE in Figure 3A, lanes 7-9 (the mock purification had no activity).

(C) Immunodepletion of p82. Unbound flow-through (FT) and bound fractions from immunodepletion with preimmune or p82 antibody serum were assayed for telomerase activity.

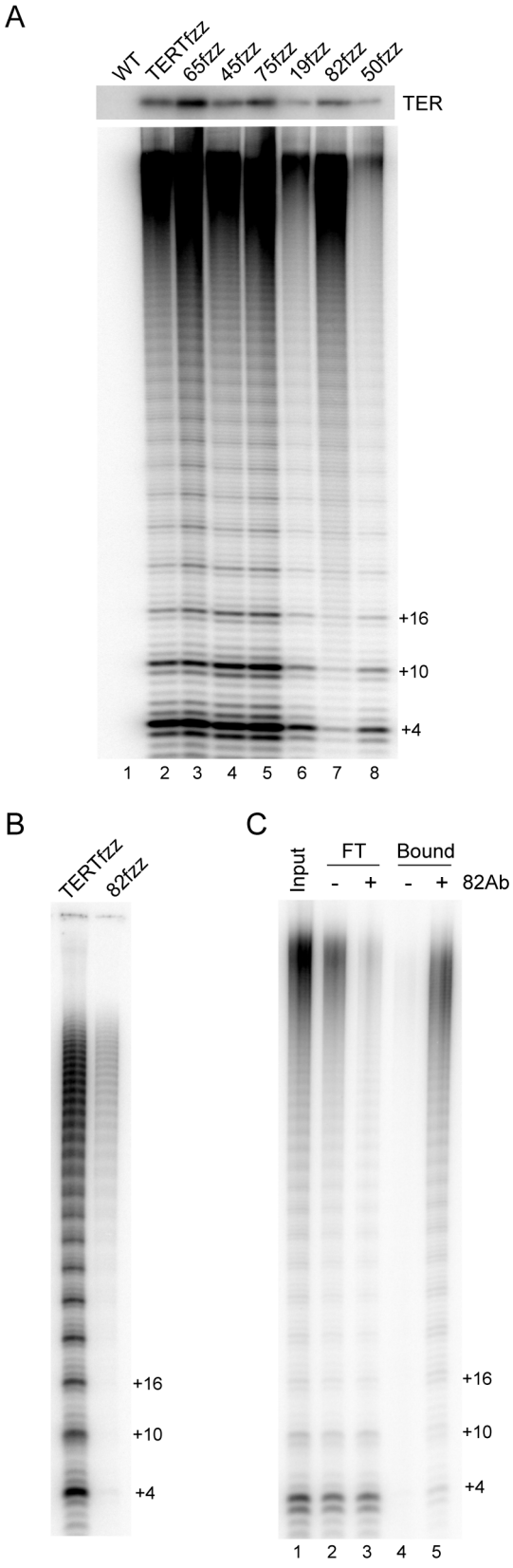
A
WT
TERTfzz
65fzz
45fzz
75fzz
19fzz
82fzz
50fzz
TER
+16
+10
+4
1 2 3 4 5 6 7 8
B
TERTfzz
82fzz
+16
+10
+4
C
Input
FT
Bound
- + - + 82Ab
+16
+10
+4
1 2 3 4 5

Figure 6. Recombinant p82 Confers Processivity to Telomerase Holoenzyme and Binds Telomeric ssDNA

(A) Purification of r82. N-terminally 6xHis-tagged r82 was stained with Coomassie Blue R-250. An open arrowhead marks the recombinant protein.

(B) Assembly of r82 with purified holoenzyme. Extra staining in the 25-32 kDa region derives from blocking proteins in the wash buffer.

(C) Activity assay of holoenzyme with or without added r82.

(D) Chase assay to establish RAP. Telomerase was preincubated with r82 (25 nM) and primer (50 nM) before the addition of nucleotides. After 10 min samples without chase were stopped, while samples with chase were supplemented with 100-fold excess unlabeled dGTP followed by another 10 min extension.

(E) DNA binding activity of r82. Fluorescein-labeled substrates NT (6FAM-$(A_2T)_6$), TeloC3 (6FAM-$(C_4A_2)_3$), TeloG3 (6FAM-$(T_2G_4)_3$), and dsTelo3 (TeloC3 annealed with unlabeled TeloG3) were incubated at 10 nM final concentration with 0, 5, or 100 nM r82.

(F) Competition assay for DNA binding specificity. The 6FAM-TeloG3 probe (10 nM) and r82 (5 nM) were bound with or without competitor oligonucleotides (1, 5, 25-fold excess over probe).

(G) Binding affinity of r82. Radiolabeled TeloG3-NT6 or NT6-TeloG3 (1 pM) was incubated with r82 (4-fold concentrations steps from 2 to 2000 pM).

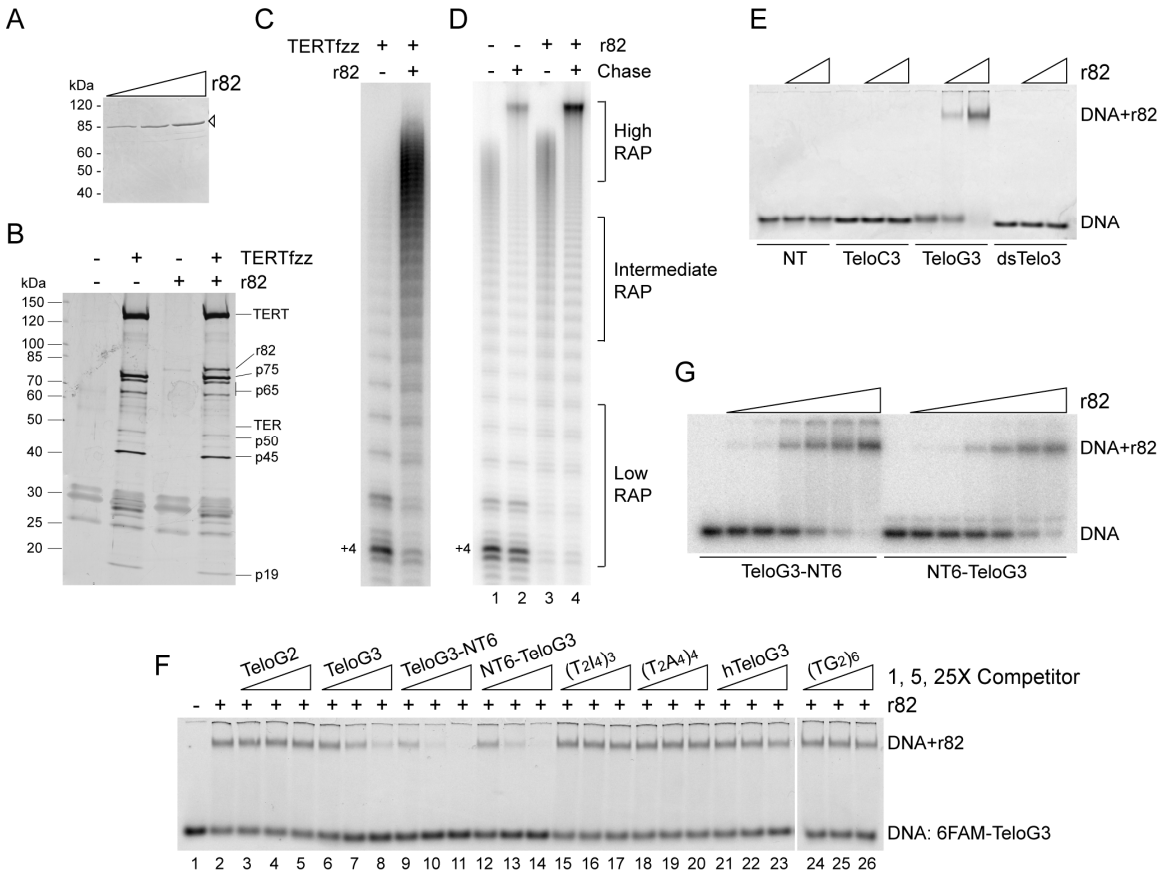
A
kDa
120
85
60
50
40
r82
B
TERTfzz
r82
kDa
150
120
100
85
70
60
50
40
30
25
20
TERT
r82
p75
p65
TER
p50
p45
p19
C
TERTfzz
r82
+4
D
r82
Chase
High RAP
Intermediate RAP
Low RAP
+4
1 2 3 4
E
r82
DNA+r82
DNA
NT
TeloC3
TeloG3
dsTelo3
G
r82
DNA+r82
DNA
TeloG3-NT6
NT6-TeloG3
F
TeloG2
TeloG3
TeloG3-NT6
NT6-TeloG3
(T2I4)3
(T2A4)4
hTeloG3
(TG2)6
1, 5, 25X Competitor
r82
DNA+r82
DNA: 6FAM-TeloG3
1 2 3 4 5 6 7 8 9 10 11 12 13 14 15 16 17 18 19 20 21 22 23 24 25 26

Figure 7. Overexpression of p82 or p50 Affects Holoenzyme Composition and Telomere Length

(A) Strategy for construction of cell lines overexpressing p82 or p50 in a TERTfzz background.

(B) Holoenzyme purification from cells overexpressing p82 or p50. Two-step affinity purification of TERTfzz was performed from extracts of cells harvested 3 h after addition of 1 μg/mL $CdCl_2$.

(C) Telomere length in bm82 and bm50 cell lines. Cells were cultured for the indicated number of population doublings (PDL) at 30°C with or without 0.1 μg/mL $CdCl_2$. Southern blots were performed using an rDNA subtelomeric probe against the G-rich strand.

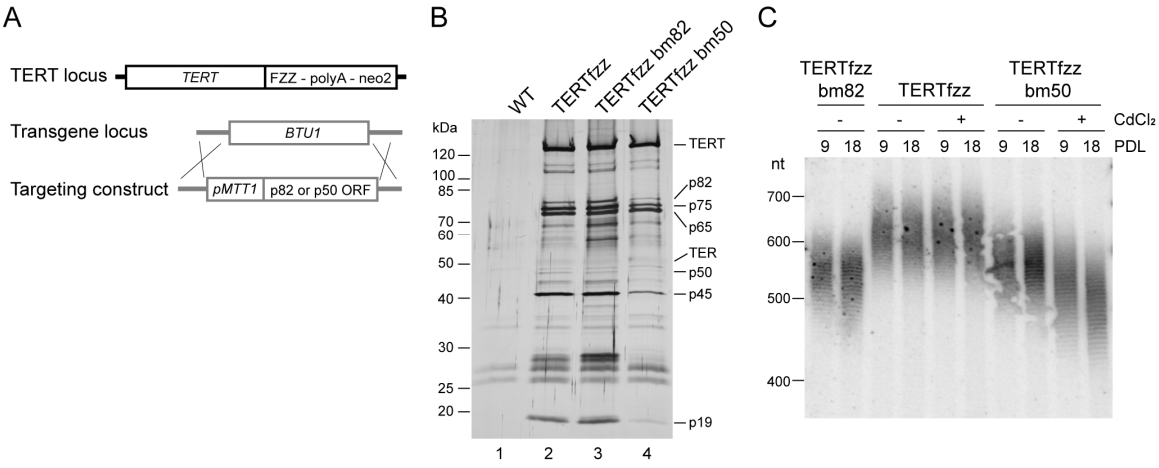
A
TERT locus
TERT
FZZ - polyA - neo2
Transgene locus
BTU1
Targeting construct
pMTT1
p82 or p50 ORF
B
WT
TERTfzz
TERTfzz bm82
TERTfzz bm50
kDa
120
100
85
70
60
50
40
30
25
20
TERT
p82
p75
p65
TER
p50
p45
p19
1
2
3
4
C
TERTfzz bm82
TERTfzz
TERTfzz bm50
-
-
+
-
+
CdCl2
9 18 9 18 9 18 9 18 9 18
PDL
nt
700
600
500
400

Supplemental Table 1. Sequence of oligonucleotides.

Notation	Oligonucleotide	Sequence (5'-3')
	$(GT_2G_3)_3$	GTTGGGGTTGGGGTTGGG
6FAM-NT	6FAM-$(AAT)_6$	6FAM-AATAATAATAATAATAAT
6FAM-TeloC3	6FAM-$(C_4A_2)_3$	6FAM-CCCCAACCCCAACCCCAA
6FAM-TeloG3	6FAM-$(T_2G_4)_3$	6FAM-TTGGGGTTGGGGTTGGGG
dsTelo3	6FAM-$(C_4A_2)_3$ and $(T_2G_4)_3$ annealed	
TeloG2	$(T_2G_4)_3$	TTGGGGTTGGGG
TeloG3	$(T_2G_4)_3$	TTGGGGTTGGGGTTGGGG
TeloG3-NT6	$(T_2G_4)_3$TATCGA	TTGGGGTTGGGGTTGGGGTATCGA
NT6-TeloG3	TATCGA$(T_2G_4)_3$	TATCGATTGGGGTTGGGGTTGGGG
hTeloG3	$(TAG_3T)_3$	TAGGGTTAGGGTTAGGGT
	$(TG_2)_6$	TGGTGGTGGTGGTGGTGG

Supplemental Figure 1. Telomerase p82 is Similar to RPA1.

(A) 3D-Jury structure prediction analysis of p82. The top five J-score predictions are shown.

(B) Primary sequence homology between predicted OB-fold domains in p82 and the OB-fold DNA-binding domains (DBD-A, DNA-B, DNA-C) of human RPA1 (hRPA1). Percent identity and additional similarity were calculated using ClustalW.

(C) Primary sequence identity comparison between p82, *T. thermophila* (Tt) RPA1, and hRPA1.

A

3D-Jury Analysis of p82

Model	J-score	PDB Hit
PSIB_01	136.50	1fgu - ssDNA-binding domain of the large subunit of RPA
PSIB_02	112.25	1l1o - Structure of the human RPA trimerization core
FFA3_02	107.75	1fgu - ssDNA-binding domain of the large subunit of RPA
FFA3_01	104.75	1jmc - ssDNA-binding domain of human RPA (183-420) bound to ssDNA
BASI_01	101.75	1fgu - ssDNA-binding domain of the large subunit of RPA

B

Comparison of OB folds in p82 and hRPA1

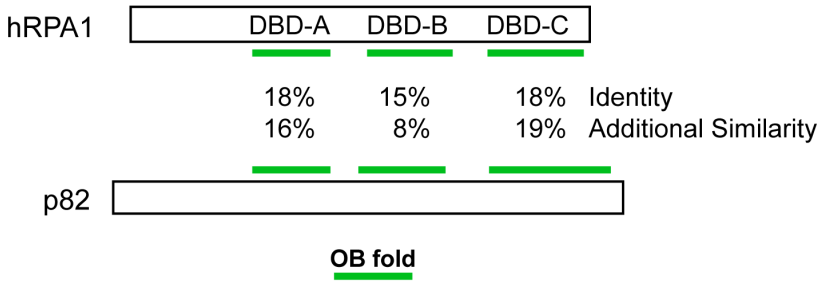

C

Primary Sequence Identity

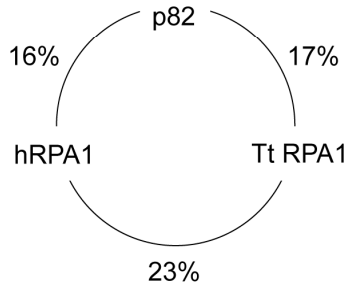

Supplemental Figure 2. *TAP19*, *TAP50*, *TAP82,* and *TAP75* can be Targeted for Expression of C-terminally Tagged Proteins.

(A) Diagram of FZZ-tagging strategy.

(B) FZZ cassette integration status. Southern blots were performed on genomic DNA using a probe that recognizes DNA fragments of different sizes for endogenous (WT) and recombinant (neo2) chromosomes. Several independent clonal cell lines were examined for each targeting.

(C) Telomere length of rDNA chromosomes. Denaturing Southern blots were performed using a subtelomeric probe against the C-rich telomeric-repeat strand. For each targeting, a selected bulk population (P) and one clonal line derived from it (C) were examined.

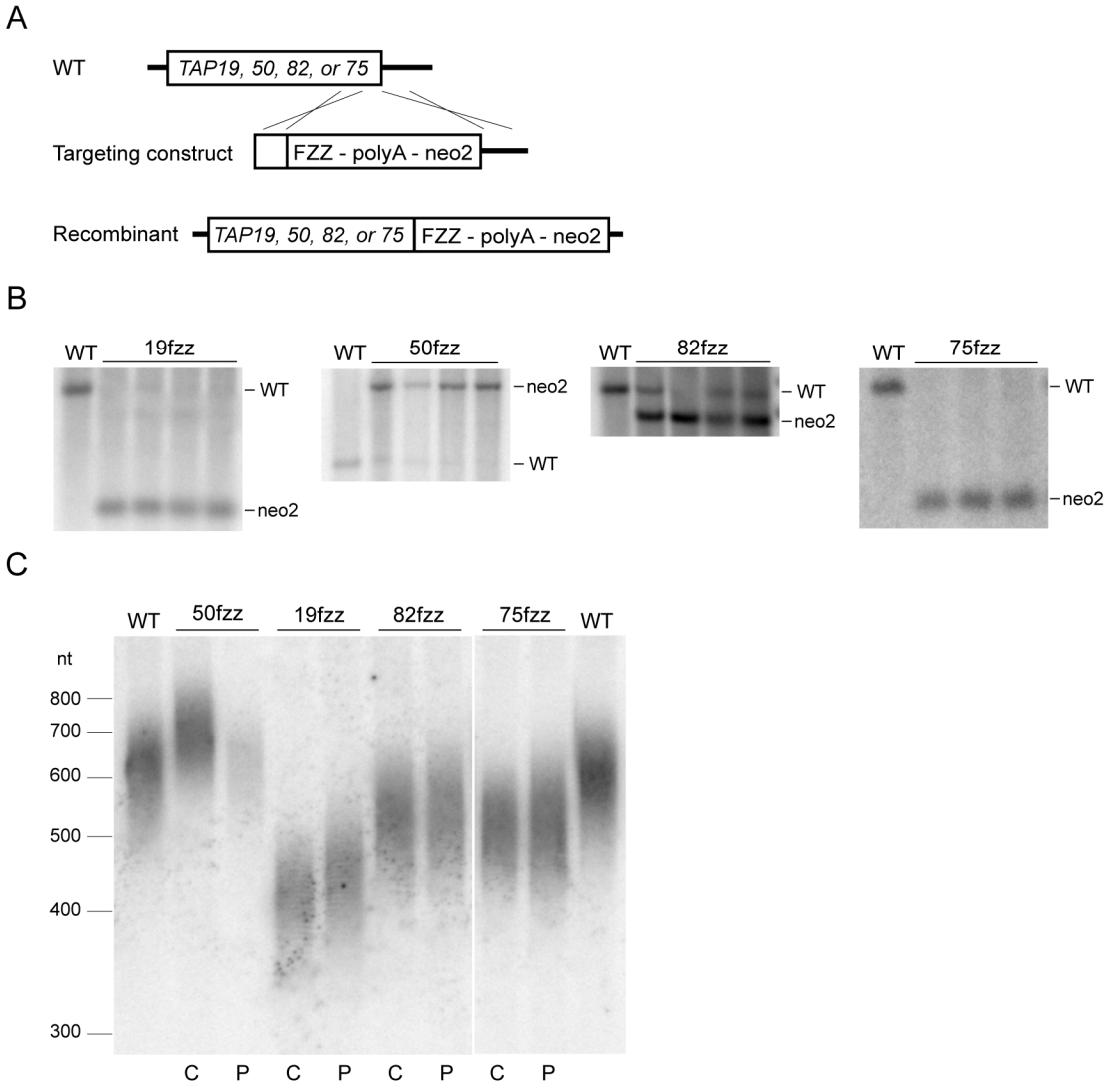
A
WT
TAP19, 50, 82, or 75
Targeting construct
FZZ - polyA - neo2
Recombinant
TAP19, 50, 82, or 75
FZZ - polyA - neo2
B
WT
19fzz
WT
neo2
WT
50fzz
neo2
WT
WT
82fzz
WT
neo2
WT
75fzz
WT
neo2
C
WT
50fzz
19fzz
82fzz
75fzz
WT
nt
800
700
600
500
400
300
C
P
C
P
C
P
C
P

Supplemental Figure 3. Tagged Telomerase Holoenzyme Proteins Copurify Other Holoenzyme Proteins, with an RNase-resistant p75-p45-p19 Subcomplex.

(A) Telomerase subunit association. Rapid single-step purification using FLAG antibody resin was carried out as in Figure 5A and analyzed by immunoblots (IB) for p65, p75, p45, and p19. TER was monitored to normalize for telomerase RNP recovery.

(B) Telomerase subcomplex association. Holoenzyme purification and RNase A treatment were performed as described for the experiment shown in Figure 4A, followed by immunoblot and Northern blot assays as in (A).

A

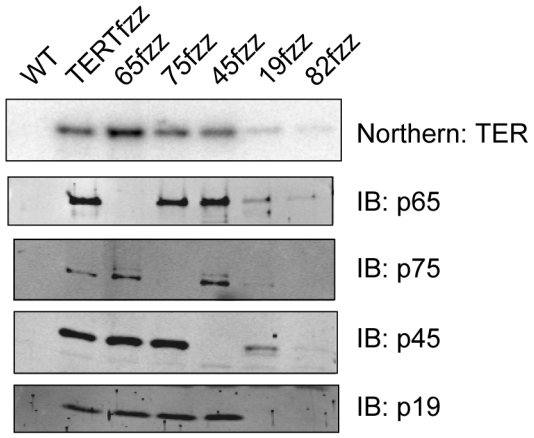
WT
TERTfzz
65fzz
75fzz
45fzz
19fzz
82fzz
Northern: TER
IB: p65
IB: p75
IB: p45
IB: p19

B

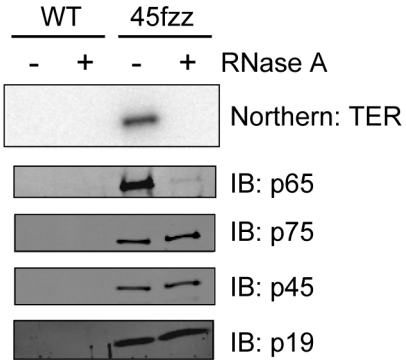
WT
45fzz
- + - + RNase A
Northern: TER
IB: p65
IB: p75
IB: p45
IB: p19

Supplemental Figure 4. Purification of 82fzz Enriches the High-RAP Fraction of the TERTfzz Holoenzyme Population.

Time course of activity assay reactions. TERTfzz holoenzyme was single-step purified on FLAG antibody resin for reactions performed using 25 nM primer.

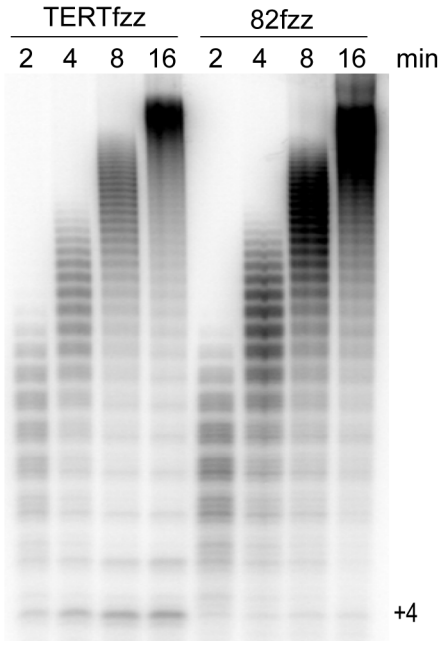
TERTfzz
82fzz
2 4 8 16 2 4 8 16 min
+4

Supplemental Figure 5. High-RAP Activity is Affected by Extract Production and r82.

(A) Variable RAP of telomerase activity purified using extracts made under different conditions. Low-speed extracts were made with or without reducing agent (DTT), protease inhibitor cocktail (PIC), and addition of a proteasome inhibitor (MG132), followed by single-step purification of TERTfzz on FLAG antibody resin.

(B) Telomerase activity with r82 titration. Telomerase activity enriched by single-step purification of TERTfzz on IgG resin was assayed using 50 nM primer and the indicated concentration of r82. When r82 is added in molar excess to DNA primer in the activity assay reaction, r82 not bound to primer competes with telomerase product DNA binding. Activity and processivity both decrease due to this competition in vitro.

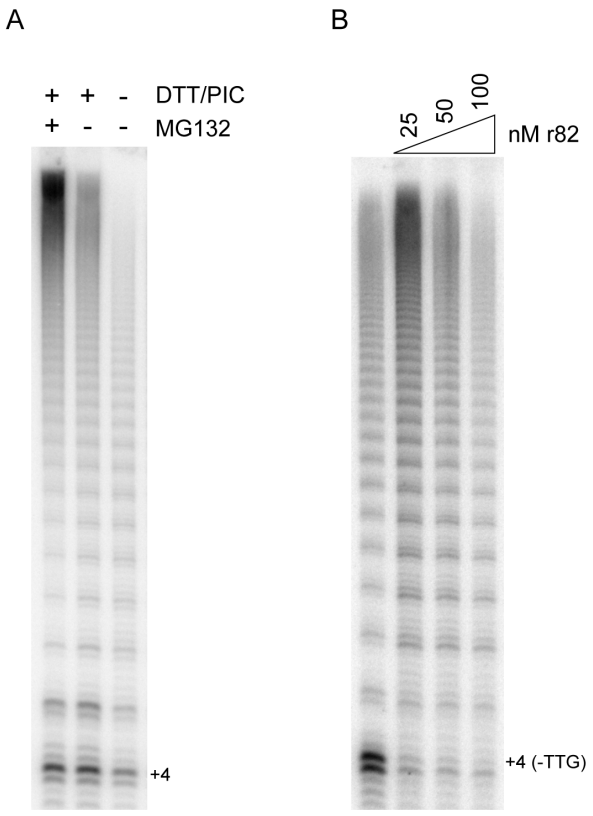
A
+ + - DTT/PIC
+ - - MG132
+4
B
25
50
100
nM r82
+4 (-TTG)

Supplemental Figure 6. Recombinant p82 Preferentially Binds a Long Telomeric Sequence.

A gel mobility shift assay was performed with 100- or 500-fold excess of competitor oligonucleotide.

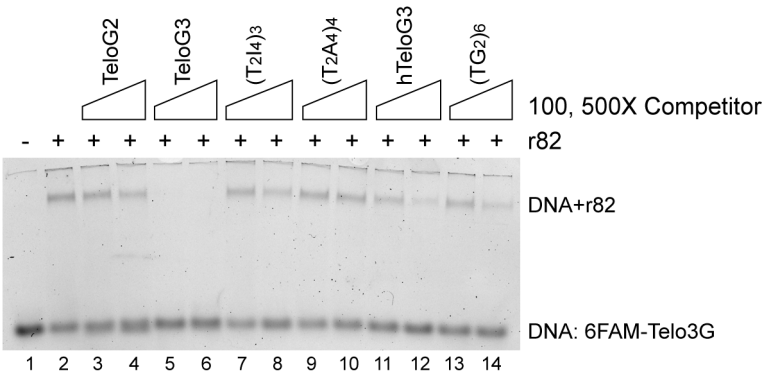
TeloG2
TeloG3
(T2I4)3
(T2A4)4
hTeloG3
(TG2)6
100, 500X Competitor
- + + + + + + + + + + + + +
r82
DNA+r82
DNA: 6FAM-Telo3G
1 2 3 4 5 6 7 8 9 10 11 12 13 14

CHAPTER THREE

RPA1-like OB folds in Teb1 Provide the Mechanistic Basis for Telomerase Processivity

Abstract

Telomerase maintains telomeres by adding telomeric repeats. The core reverse transcriptase of telomerase activity can be reconstituted *in vitro* by just telomerase reverse transcriptase (TERT) and telomerase RNA (TER). Endogenously assembled telomerase holoenzymes contain additional proteins that are essential for telomerase function *in vivo*. In *Tetrahymena thermophila*, holoenzyme proteins include an RPA1-like subunit with telomeric single-stranded DNA (ssDNA)-binding activity (p82, here termed Teb1) and a three-protein Telomere Adaptor Subcomplex (TASC) that links Teb1 to the catalytic core. We compared the properties of *T. thermophila* RPA1 (Rpa1) and Teb1. Teb1 has specificity for telomeric ssDNA and confers high repeat addition processivity (RAP) to telomerase while Rpa1 binds without specificity and does not affect RAP. However, an important factor for telomerase RAP is the OB fold in Teb1 that connects the two ssDNA-binding OB folds to TASC. Chimeric protein made from Teb1 and Rpa1 shows that sequence-specificity in DNA-binding is not important for high RAP. Our study reveals a mechanism for telomerase processivity that involves multiple protein subunits and RPA1-like OB-folds.

Introduction

Telomerase maintains chromosome ends by synthesizing telomeric repeats. Telomerase reverse transcriptase (TERT) catalyzes telomeric repeat addition to the 3' ends of the chromosomes using the template region of telomerase RNA (TER). Telomerase activity is highly regulated at the cell-cycle level and restricted to S phase. Telomerase is also regulated at the developmental level. For example, in multicellular organisms, telomerase expression and activity are limited to cell lineages that need to maintain their long-term proliferative potential. Most cancer cells aberrantly activate telomerase and telomere maintenance, in order to divide indefinitely (Forsyth et al., 2002).

To gain insight into how telomerase and telomeres are regulated, one approach is to study telomerase-associated proteins and how they affect telomerase activity. Studies in the ciliate *Tetrahymena thermophila* initially uncovered telomerase activity (Greider and Blackburn, 1985), and *T. thermophila* telomerase enzyme biochemistry has been characterized extensively, using both the endogenous holoenzyme and the TERT·TER minimal RNP that is reconstituted *in vitro* (Blackburn et al., 2006) (Collins, 1999). Endogenous telomerase holoenzyme displays low and high repeat addition processivity (RAP). Low RAP and high RAP activity give rise to short and long primer extension products, respectively. However, only low RAP activity is observed in the reconstituted minimal RNP (Hardy et al., 2001). High RAP activity has been attributed to telomerase complex that has very low dissociation rate from its substrate (Greider, 1991), and this

was proposed to be from an anchor site within TERT and/or TERT-associated protein(s) (Collins and Greider, 1993; Lee and Blackburn, 1993).

In addition to TERT and TER, *T. thermophila* telomerase has six components: p65, p75, p45, p19, p82, and p50 (Min, 2009; Witkin and Collins, 2004; Witkin et al., 2007). TER-binding protein p65 is involved in telomerase RNP biogenesis. Three subunits p75, p45, and p19 form the Telomeric Adaptor Subcomplex (TASC). Regulatory subunit p50 is likely to be a chaperone for TASC assembly with the minimal RNP. TASC recruits p82 into the complex. We have demonstrated that p82 is required for high RAP activity of endogenous telomerase complex (Min, 2009). Because p82 binds telomeric single-stranded DNA (ssDNA) and contributes to the telomerase anchor site, we now rename it Teb1 and the gene *TEB1*, for Telomere Binding 1.

Teb1 shares sequence similarity with RPA1, the largest subunit of the Replication Protein A (RPA) heterotrimeric complex (Min, 2009). However, TEB1 is not the *T. thermophila* RPA1 gene: *T. thermophila* genome encodes RPA1-like *TEB1* and *RPA1* genes. RPA functions in general DNA replication, DNA recombination, and DNA repair pathways (reviewed in (Wold, 1997)). Moreover, RPA has also been implicated in regulating telomerase activity (Schramke et al., 2004). Both telomerase activity enhancement and inhibition by RPA have been reported (Cohen et al., 2004; Rubtsova et al., 2009). The enhancement of telomerase activity may arise from the disruption of inhibitory structures that can form on repetitive G-rich ssDNA (Salas et al., 2006). If this is the mechanism of telomerase processivity, then *T. thermophila* Rpa1 may have similar effect as Teb1.

In this study, we investigated the mechanism of Teb1-mediated telomerase high RAP, initially by comparing Teb1 and *T. thermophila* Rpa1. Although both Teb1 and Rpa1 show similar biochemical activity except for the telomeric sequence-specificity of Teb1, only Teb1 increases telomerase high RAP. Teb1 contributes to telomerase much more than the disruption of possible substrate structures, and the mechanism of high RAP involves multiple telomerase-associated proteins. We show that telomerase high RAP involves Teb1 and TASC, and these proteins associate through the C-terminal OB fold in Teb1. *T. thermophila* telomerase processivity is accomplished by increasing the association of the enzyme activity with substrate DNA, using RPA1-like OB folds.

Results

Functional Comparison of T. thermophila *Teb1p and Rpa1p*

RPA complex has four DNA-binding (DBD) OB folds, three of which are found within RPA1 (reviewed in (Bochkarev and Bochkareva, 2004)). RPA1 can be divided into four domains, each with one OB fold: N, DBD-A, DBD-B, and DBD-C (Figure 1A). N domain is not required for DNA-binding (Gomes and Wold, 1996), and the three DBDs bind ssDNA. DBD-C also participates in the trimerization of RPA complex and contains a Zinc binding motif. Zinc is thought to contribute to the RPA structure and not the ssDNA-binding activity. *T. thermophila* telomerase subunit Teb1 shares similarity to RPA1, in the OB folds and the predicted domain organization (Min, 2009). Teb1 was aligned with *T. thermophila* Rpa1, and the protein domains were designated as N, DBD-A, DBD-B, and DBD-C, to reflect the similarity between the two proteins (Figure 1A).

RPA1 has been studied biochemically in human and yeast systems, but not in *T. thermophila*. Therefore, we aimed to compare *T. thermophila* Rpa1 with Teb1, especially in the context of telomerase. We first assessed the essential function of *RPA1*, but our efforts to make knockdown strain were unsuccessful, likely due to high gene expression requirement. We also tried to confirm the expected RPA heterotrimer, but the endogenous CT tagging strategy for *RPA1* disrupted functional complex formation (data not shown). We next attempted to express Rpa1 recombinantly in *E. coli*. Like the recombinant Teb1, the recombinant Rpa1 alone without the other subunits was soluble (Figure 1B). This allowed us to perform comparisons of their biochemical properties.

We first assessed the ssDNA-binding activities of the recombinant Teb1 and Rpa1 proteins with electrophoretic mobility shift assays (EMSA). As shown previously, Teb1 binds telomeric ssDNA but not non-telomeric ssDNA (Figure 1C) (Min, 2009). Rpa1 bound both telomeric and non-telomeric ssDNA substrates (Figure 1C). Rpa1 bound with similar affinity to telomeric and non-telomeric substrates with lower affinity than Teb1 for telomeric ssDNA, consistent with a general ssDNA-binding activity found in human and yeast RPA1.

We also compared the dissociation rates of Teb1 and Rpa1. Teb1 and Rpa1 were first bound to radiolabeled probes, then challenged with excess unlabeled probe (for Teb1) or with dilution to below Kd (for Rpa1). DNA-protein complexes were analyzed over time by EMSA. Dissociation of DNA-protein complexes results in the disappearance of shifted band and the appearance of free probe, and the shifted bands are completely gone within a few minutes (Figure 1D). Thus, ssDNA complex formed by either protein dissociate fast enough to be completely dissociated within few minutes, even at 4°C. To summarize, *T. thermophila* Rpa1 displays the characteristics expected from a subunit of the RPA complex. Like Teb1, Rpa1 can interact with telomeric ssDNA. Unlike Teb1, Rpa1 can also interact with nontelomeric ssDNA.

Although Rpa1 can bind telomeric ssDNA, it may not have similar impact as Teb1 on telomerase high RAP. We have shown previously that endogenous telomerase purified by tagged TERT displays both low and high RAP, due to substoichiometric association of Teb1 (Min, 2009). Addition of recombinant Teb1 to the TERT-purified, mixed population telomerase increases the amount of high RAP (Min, 2009). To determine whether high RAP stimulation requires only a ssDNA-binding factor to coat

the substrate primer, Teb1 or Rpa1 was added to TERT-purified telomerase and assayed for telomerase activity by telomeric primer extension. In reactions with Teb1, the increase in high RAP is evident from the increase in longer product accumulation (Figure 1E). In contrast, Rpa1 had little effect on telomerase activity (Figure 1E, compare lane 1 to lanes 7-11). Interestingly, a high ratio of Teb1 to oligonucleotide substrate inhibited product synthesis and high RAP in particular (Figure 1E, lane 6). Higher ratio of Rpa1 to substrate caused overall inhibition of telomerase activity without any stimulation of high RAP (data not shown). Inhibition of telomerase activity by the presence of ssDNA-binding proteins in excess over substrate DNA is most likely due to competition for substrate binding between TERT and the ssDNA-binding proteins.

Telomeric ssDNA Permutation and Length Requirements for Binding by Teb1

Both Teb1 and Rpa1 bind telomeric ssDNA, but only Teb1 conferred an increase in telomerase high RAP. We therefore turned our attention to Teb1 DNA-binding activity in more detail to understand the mechanism behind how Teb1 confers high RAP.

Teb1 binds specifically to telomeric ssDNA and does not have discernable affinity for nontelomeric ssDNA (Min, 2009). Teb1 does not require the telomeric sequence to be at the 3' end of ssDNA, consistent with its function as a telomerase protein and not a telomere end-binding protein. Teb1 also preferentially binds longer (3 repeat) telomeric ssDNA over shorter ones (2 repeat).

Here, in an attempt to avoid the presence of multiple binding sites in a single substrate, we used 2 repeat telomeric ssDNA and asked whether Teb1 prefers certain telomeric sequence permutation. Telomeric 2-repeat oligonucleotides of all six

permutations were tested by EMSA. Teb1 bound these substrates with varying affinities, which can be estimated by the concentration of Teb1 that shifted half of the free ssDNA (Figure 2A). Teb1p preferred the $(G_3T_2G)_2$ permutation and had the lowest affinity for the $(T_2G_4)_2$ permutation. We noted supershifts of DNA-protein complex migration near or at the wells with ssDNA that were bound with higher affinity by Teb1 (Figure 2A). The supershifted bands suggested that with certain permutations, multiple proteins may be able to occupy a relatively short 12-mer oligonucleotide.

We next tested oligonucleotide substrates ranging in length from 10 to 18 nucleotides, keeping the 5' end permutation fixed with the preferred permutation G_3T_2G (Figure 2B). Once again, we noted supershifted bands that become more evident as the substrate increases in length (Figure 2B). Because of variable migration of bound ssDNA, all affinity calculations were done by measuring the disappearance of free ssDNA. The affinity for 18-mer substrate was about 100-fold higher than the affinity for 10-mer substrate (Figure 2C). A big step change in Kd is expected from the creation of a new binding site, but with each nucleotide length change from 18 to 10 nt, Kd shifted in small steps (Figure 2C). This suggested that Teb1 recognition and binding is adaptable to the available sequence.

In Vitro *Reconstitution of Telomerase Complex with High RAP*

The function of Teb1 in conferring high RAP to telomerase was shown previously by adding recombinant Teb1 to TERT-purified, mixed population telomerase. In this system, the mixture of low, intermediate, and high RAP even before the addition of Teb1 limited our detection of changes in intermediate RAP.

In order to better study Teb1-dependent telomerase processivity, we set up a telomerase reconstitution system that would depend solely on the recombinant Teb1 for high RAP activity. Telomerase core RNP composed of TERT and TER or TERT, TER, and p65 can be made heterologously using rabbit reticulocyte lysate (RRL) *in vitro* transcription/translation. The RRL-reconstituted core RNP complex displays only low RAP (Prathapam et al., 2005), so we sought to build it up with additional telomerase-associated proteins. Previously, we found that TASC (p75-p45-p19) is required to bridge Teb1 to the core RNP (Min, 2009). We have not yet been able to reconstitute TASC from recombinant subunits. However, *T. thermophila* TASC can be purified apart from the catalytic core by using RNase to degrade TER (Min, 2009). TER-degradation disrupts TERT folding and releases TASC from TERT, TER, and p65. We attempted to reconstitute a telomerase complex with high RAP using three different subcomponents (core RNP, TASC, Teb1) made in three different systems (Figure 4A).

To obtain TASC, we purified epitope-tagged p45 (45fzz) (Min, 2009) and treated with microccocal nuclease. Robust nuclease treatment and stringent washing before peptide elution yielded mostly TASC without active TERT and very little if any Teb1 (Figure 4B). We tested the purified TASC in telomerase assay to ensure that the small fraction of TERT carryover (Figure 4B), likely as unfolded protein, is indeed inactive (data not shown). We then combined TASC and/or Teb1 with TERT·TER or TERT·TER·p65 core RNP assembled in RRL, then assayed for telomerase activity (Figure 3C). The control samples had mock addition of TASC and/or Teb1 buffers to match the salt concentration. Because telomerase activity is inhibited by salt, TERT·TER or TERT·TER·p65 core RNP alone had low activity: only two repeat additions were

readily detected (Figure 3C, lanes 1 and 5). Addition of Teb1 without TASC did not change telomerase activity, as expected (Figure 3C, lanes 2 and 6).

Curiously, the addition of TASC improved overall activity of the enzyme (Figure 3C, lanes 3 and 7). Our TERT·TER or TERT·TER·p65 recombinant core RNP showed similar product profile when assayed without salt (data not shown). Therefore, TASC improved telomerase activity without improving RAP. We suspect that the association of telomerase core with TASC protects the RNP or the RNP·DNA complex from the adverse effects of salt.

The combination of telomerase core, TASC, and Teb1 resulted in the successful reconstitution of high RAP (compare Figure 3C, lanes 4 and 8 to Figure 1E, lane 1). This is the first report of *in vitro* reconstitution of high RAP telomerase activity. From this experiment, we conclude that telomerase catalytic core made in RRL is capable of high RAP. Also, high RAP reconstitution confirms the requirement of TASC to bridge the core to Teb1 (as diagrammed in Figure 3A). This reconstitution system allows the discrimination of Teb1 function in high RAP without the background of mixed telomerase population present in endogenous telomerase purifications. Because p65 was not essential for high RAP, subsequent reconstitution experiments were carried out with telomerase core RNP made up of TERT and TER.

Analysis of Teb1 Domain Requirements for Telomerase High RAP

In order to address which domain(s) of Teb1 contributed to telomeric ssDNA-binding and which contributed to high RAP, we made domain truncations of Teb1 (Figure 3A). The domains that contained DBD-A, DBD-B, and DBD-C OB folds were

designated as N, A, B, and C. Truncation from either the N-terminus or the C-terminus was used to create various forms of Teb1: N, NA, NAB, A, AB, ABC, B, BC, and C. The truncated proteins were expressed in *E. coli* and purified (Figure 3B).

EMSA using Teb1 truncation proteins showed that A and B domains bind telomeric ssDNA while N and C domains do not (Figure 3C). Any truncated protein that included either the A or the B domain bound telomeric ssDNA. We found that even 15 μM of $Teb1^{C}$ did not show any ssDNA-binding activity by EMSA (data not shown). Unlike the DBD-C of RPA1, $Teb1^{C}$ may not interact with ssDNA. Therefore, there are two telomeric ssDNA-binding OB folds in Teb1.

Telomerase complex reconstitution was used to test the effect of Teb1 truncations on telomerase activity. We supplemented the catalytic core RNP with purified TASC and Teb1 truncation proteins before assaying for activity (Figure 4D). Only $Teb1^{ABC}$ and $Teb1^{BC}$ proteins conferred high RAP to telomerase; their effect was comparable to that of the full-length protein, $Teb1^{FL}$ (Figure 4D, lanes 2-3, 14-15, 18-19). In contrast, proteins that lacked the C domain had little to no effect on telomerase activity (Figure 4D, lanes 4-13, 16-17). These results indicate that the C domain is necessary for bridging the ssDNA-binding activity of the A and B domains to the telomerase complex. Without this protein-protein connection, ssDNA-binding activity is uncoupled from other telomerase subunits and high RAP is not conferred. $Teb1^{AB}$ inhibited telomerase activity at the higher concentration tested. Similar activity inhibition was observed with excess $Teb1^{FL}$ (Figure 1E, lane 6), as reported previously for holoenzyme assays (Min, 2009). Because $Teb1^{BC}$ also confers high RAP, the minimal Teb1 requirement for high RAP is the C domain connected to one ssDNA-binding domain.

C domain alone stimulated some high RAP of the reconstituted telomerase, at the higher concentration tested (Figure 4D, lanes 20-21). The effect of $Teb1^{C}$ is more pronounced on the shorter products (low RAP) than on the longer products (intermediate and high RAP). In contrast, $Teb1^{FL}$, $Teb1^{ABC}$, and $Teb1^{BC}$ primarily increase high RAP. These differences in telomerase activity suggest that the mechanism behind $Teb1^{C}$ is likely different from a version of Teb1 protein with ssDNA-binding activity. $Teb1^{C}$ may change the core·TASC conformation or may have some DNA-binding activity in the context of the TASC and the catalytic core. For example, the RPA complex has been observed to change conformation, depending on the ssDNA substrate length (Bochkareva et al., 2002).

$Teb1^{C}$-Mediated Activation of RPA1 DNA-Binding Domains to Confer High RAP

Because $Teb1^{C}$ in conjunction with DNA-binding is necessary for high RAP, we next analyzed the C domain of Teb1 in more detail. In the crystal structure of the RPA trimerization core, the C-terminal αhelix peptide of RPA1 is used to interact with RPA2 and RPA3 (Bochkareva et al., 2002). To test whether Teb1 uses its CT αhelix to assemble with TASC, we made a CT peptide deletion mutant designated Teb1ΔCTαh (Figure 5A). This construct was expressed in *E. coli* and the protein was purified (Figure 5B). When tested by EMSA, Teb1ΔCTαh bound telomeric ssDNA (Figure 5C). In our reconstituted telomerase complex activity assay, Teb1ΔCTαh stimulated high RAP, similarly to $Teb1^{FL}$ (Figure 5D, lanes 2-5). We conclude that Teb1 does not require the CT αhelix to assemble with other subunits.

We next addressed whether the sequence specificity of ssDNA-binding activity in Teb1 was important for conferring high RAP to telomerase. We took advantage of the similarity between Rpa1 and Teb1 to make a protein with Rpa1-like ssDNA-binding activity and Teb1-like TASC-interacting activity. In this chimeric protein, $Rpa1^{NAB}$-$Teb1^{C}$, the NAB domains of Rpa1 were fused to the C domain of Teb1 (Figure 5A). We reasoned that as long as the ssDNA-binding activity is connected to telomerase through the TASC-interacting domain, even Rpa1 may confer high RAP to telomerase. If sequence-specificity of Teb1 is important for high RAP, then $Rpa1^{NAB}$-$Teb1^{C}$ would be unable to fulfill the role of Teb1, and the effect of $Rpa1^{NAB}$-$Teb1^{C}$ should be similar to $Teb1^{C}$.

We tested the retention of RPA1 DNA-binding activity in the chimeric protein using EMSA. As predicted, $Rpa1^{NAB}$-$Teb1^{C}$ bound both telomeric and nontelomeric ssDNA substrates, just like Rpa1 (Figure 5C). This chimeric protein was reconstituted with the core and TASC, and the reconstituted telomerase was assayed for the ability to stimulate RAP. Unlike $Rpa1^{FL}$, $Rpa1^{NAB}$-$Teb1^{C}$ chimera conferred high RAP (Figure 5D, lanes 8-11). Moreover, high RAP conferred by $Rpa1^{NAB}$-$Teb1^{C}$ is much more than that conferred by $Teb1^{C}$; the effect of $Rpa1^{NAB}$-$Teb1^{C}$ is very similar to high RAP conferred by $Teb1^{FL}$ (Figure 5D, lanes 2-3, 6-9). These results suggest that the coupling of ssDNA-binding activity and telomerase through the unique OB fold in $Teb1^{C}$ is sufficient for high RAP.

Discussion

In this study, we have refined the model of *T. thermophila* telomerase complex architecture and its interaction with telomeric ssDNA substrate. Moreover, our work presented here illuminates the mechanism behind telomerase high repeat addition processivity. Like the sliding clamp which confers processivity to DNA polymerases by decreasing the enzyme-substrate dissociation, Teb1 confers processivity to telomerase by increasing telomerase association with substrate. Interestingly, although only one telomerase subunit has RPA1-like ssDNA-binding activity, this subunit requires three additional proteins that form the bridge to the catalytic core. This raises the possibility that TASC, as the adaptor between Teb1 and the core RNP, is used to fine-tune telomerase activity.

We have previously defined *T. thermophila* telomerase holoenzyme as the complex that is active *in vivo*, and telomerase purification experiments suggested that the holoenzyme contains TERT, TER, p65, TASC, and Teb1 (Min, 2009). Our current model of the telomerase architecture is that the core RNP (TERT·TER·p65) assembles with TASC (p75-p45-p19), and that Teb1 associates with this core·TASC complex (Figure 6). We have successfully reconstituted telomerase complex with high RAP using three isolated telomerase subcomplexes/subunit. With this, we have now defined the minimal telomerase complex with high RAP, which consists of TERT, TER, TASC, and Teb1. Although p65 is not required for the assembly of high RAP telomerase, we did note an increase in the yield of active telomerase RNP when the core was made with p65. This was expected from the ability of p65 to improve TERT-TER assembly.

T. thermophila telomerase high processivity requires both an RPA1-like Teb1 subunit and TASC. Specifically, ssDNA-binding activity of Teb1 provides the molecular mechanism for increasing the association of telomerase substrate with the enzyme. The effect of Teb1 on *T. thermophila* telomerase complex is not a general effect of disrupting ssDNA structures as was proposed for the effect of RPA on telomerase activity in other organisms. The biochemical data suggest that Teb1 is sampling many possible binding registers on telomeric ssDNA, using two DNA-binding domains A and B. The adaptable binding of Teb1 explains the higher affinity for longer ssDNA that may provide multiple binding sites. These properties of Teb1 make sense in telomerase processivity mechanism: Teb1 can recognize variable telomeric overhang lengths and permutations found *in vivo*, but it does not tether telomerase to telomeres.

Although the ssDNA-binding activity of the A and B domains are crucial for high RAP, the C domain serves an equally essential function: the C domain links the A and B domains to telomerase catalytic core via TASC (Figure 6). Without the C domain, the ssDNA-binding activity is uncoupled from telomerase catalytic activity and telomerase does not have high RAP. However, the C domain of Teb1 is not just a simple connector of ssDNA-binding domains A and B to TASC. Incorporation of the $Teb1^{C}$ protein into the core·TASC complex improved telomerase processivity, even though $Teb1^{C}$ lacked discernable ssDNA-binding activity. Although $Teb1^{C}$ does not confer the same extent of RAP as $Teb1^{BC}$, $Teb1^{ABC}$, and $Teb1^{FL}$, it changes the activity of the core·TASC complex. In our *in vitro* reconstituted telomerase assays, we observed products ending in TGGGGT-3' permutation, in addition to the usual GGGTTG-3' permutation products (Figure 4D and Figure 5D). Similar shift in product permutation was observed with

various Teb1 truncations, but the change was most striking with Teb1^{C}. It is provocative that TGGGGT-3' is the end permutation of telomeres observed in *T. thermophila* (Jacob et al., 2001). The change in the product profile indicates that the translocation or the rate-limiting step in telomerase catalytic cycle is changed. We suspect that Teb1^{C} changes the conformation of the core·TASC complex.

It is interesting that even Teb1^{BC}, with a single ssDNA-binding domain, confers high RAP; the high RAP product accumulation and the low RAP product profile are most similar to Rpa1^{NAB}-Teb1^{C} chimera. The chimeric protein (without sequence-specifity) and the truncated Teb1^{BC} (with only one DNA-binding domain) can compensate for Teb1^{FL} and confer high RAP to telomerase. However, their effects on telomerase activity are slightly different due to the biochemical differences from Teb1^{FL}. We hypothesize that *in vivo*, telomeric sequence-specificity of Teb1 is important for binding telomeric ssDNA in the presence of other telomere-binding proteins and non-telomeric ssDNA. *T. thermophila* telomerase may have adapted an RPA1-like subunit to provide substrate binding and subsequently gained telomeric sequence-specificity for efficient recruitment to telomeres.

Same principles behind telomerase processivity may apply in other organisms. Genetic analyses have revealed the importance of coupling telomeric ssDNA-binding activity and telomerase activity. For example, budding yeasts have an RPA-like complex that exists at telomeres (Cdc13-Stn1-Ten1) (reviewed in (Haring and Wold, 2007)). Cdc13 uses OB folds to bind telomeric ssDNA. Cdc13 also stimulates telomerase activity by associating with telomerase-associated protein Est1 during S phase. In humans, POT1/TPP1 complex, which binds telomeric ssDNA, stimulates telomerase activity

(Wang et al., 2007; Xin et al., 2007). Thus, in various organisms, telomere-binding activity is used to regulate telomerase activity, and their mechanism of action may be similar to Teb1 and TASC.

Our study highlights the importance of studying the telomerase holoenzyme complex to fully appreciate telomerase enzyme activity. In the *T. thermophila* system, it is now possible to reconstitute a telomerase complex with high RAP that is similar to the purified holoenzyme. Future studies, both *in vitro* and *in vivo*, may reveal the separation in the roles of Teb1 and TASC in telomerase catalytic cycle, telomerase recruitment to telomeres, and telomere elongation.

Materials and Methods

Recombinant Protein Expression and Purification

All recombinant proteins were expressed from pET28a vector (NT His_6-tagged) in BL21(DE3) cells as described for Teb1 (r82) in Chapter Two. The proteins were eluted in EB (20 mM Tris-Cl pH 8, 1 mM $MgCl_2$, 10% glycerol, 300 mM NaCl, 0.1% Igepal, 300 mM imidazole) and supplemented with 5 mM DTT before storage at -80°C. Proteins were supplemented with additional 2 mM DTT upon thawing, before use.

Teb1 truncations were cloned by PCR into pET28a vector. $Rpa1^{NAB}$-$Teb1^{C}$ chimera was also cloned by PCR, and the junction between Rpa1 and Teb1 parts of the protein contains a NheI site.

EMSA

EMSA conditions are described in Chapter Two. For the Teb1 k*off* EMSA experiment, 10 pM radiolabeled 18G3 was preincubated with 1 nM Teb1 at room temperature to bind then transferred to ice to slow the dissociation rate. Then ssDNA-Teb1 complex was challenged with 100 nM cold 18G3, which is in excess of both the hot probe and Teb1 concentrations. For the Rpa1 k*off* EMSA experiment, 1 µM Rpa1 was preincubated with 5 nM radiolabeled 18G3 or T18 and then transferred to ice. Then the ssDNA-Rpa1 complex was challenged by 100-fold dilution with binding buffer so that probe was 10 pM (far below Rpa1 Kd). Aliquots of the reactions were loaded onto prechilled native acrylamide gel before (t=0) and after the challenge (at indicated times), and electrophoresis was carried out in the cold room.

Telomerase complex and high RAP reconstitution

Telomerase core RNP was made in Promega's TNT RRL system following the manufacturer's instructions using recombinant TERT or p65 cloned into pCITE4a vector. *In vitro* transcribed TER was added to the RRL reaction at 1 ng/µl. For each assay, 25 µl of RRL reaction of TERT was immunoprecipitated with 7 µl M2 FLAG resin (Sigma) and washed into T2MG (20 mM Tris-Cl pH 8, 1 mM $MgCl_2$, 10% glycerol) supplemented with 5 mM β-mercaptoethanol (β-me).

TASC was prepared by purifying telomerase from cells expressing tagged p45 (45fzz) and described in Chapter Two. After two-step purification of 45fzz, immobilized telomerase on M2 FLAG resin was treated with 10 µl/ml MNase (NEB) in T2MG50+I (T2MG, 50 mM NaCl, 0.1% Igepal) buffer supplemented with 2 mM $CaCl_2$ and incubated at room temperature (RT) for 30 min. The reaction was stopped with 2 mM EDTA and washed for 30 min with 4 changes of T2MG50+I buffer. Then the remaining TASC was eluted with 3X FLAG peptide (Sigma) at 0.2 mg/ml concentration in T2MG50+I buffer with 2 mM DTT. Typical TASC purification contained ~ 0.2-0.5 ng/µl of each TASC subunit as determined by SDS-PAGE.

For telomerase reconstitution, RRL-made TERT purified on resin (25 µl RRL reaction and 7 µl M2 FLAG resin) was incubated with 3.5 µl purified TASC (~ 1 mM final) and indicated amounts of recombinant Teb1 or Rpa1 proteins. The control samples were incubated with matching TASC and recombinant protein buffers.

Telomerase Activity Assay

Activity assay were carried out as described in Chapter Two for purified telomerase activity. All assays were carried out by preincubating telomerase (endogenous or in *vitro* reconstituted) with substrate primer for 10 min at RT before the addition of assay buffers and nucleotides to start primer extension. Also, the assay incubation was carried out at RT instead of 30°C, for 20 min, which was enough to show the difference in high RAP and low RAP but before the longest extensions become difficult to resolve by PAGE.

For the recombinant telomerase activity assay, the conditions have been changed from the endogenous telomerase activity assay. The reaction buffer contained 50 mM Tris-Cl pH 8, 1.25 mM $MgCl_2$, 5 mM DTT, and the amount of nucleotides in the reaction included: 0.1 mM dTTP, 10 μM cold dGTP, and 0.5 μl hot [α-^{32}P]dGTP (PerkinElmer, 3000 Ci/mmol, 10 mCi/ml).

Figure 1. Teb1 and Rpa1 both bind telomeric ssDNA but only Teb1 increases telomerase high RAP.

(A) Diagram of T. thermophila Rpa1 and Teb1 proteins.

(B) Recombinant Teb1 and Rpa1. Coomassie-stained SDS-PAGE of purified NT His-tagged recombinant proteins is shown.

(C) ssDNA-binding activity of Teb1 and Rpa1. 10 pM 5'-radiolabeled 18G3 and T18 (T_{18}) oligonucleotides were used in gel shift assays with 1-625 nM protein.

(D) Fast koff of Teb1 and Rpa1 ssDNA-binding. Protein-DNA complex was challenged with excess primer (Teb1) or diluted below the Kd (Rpa1) and loaded into the gel at indicated times.

(E) Effect of Teb1 and Rpa1 on telomerase activity. 200 nM 18G3 primer and 0.32-200 nM protein were preincubated with purified telomerase then assayed.

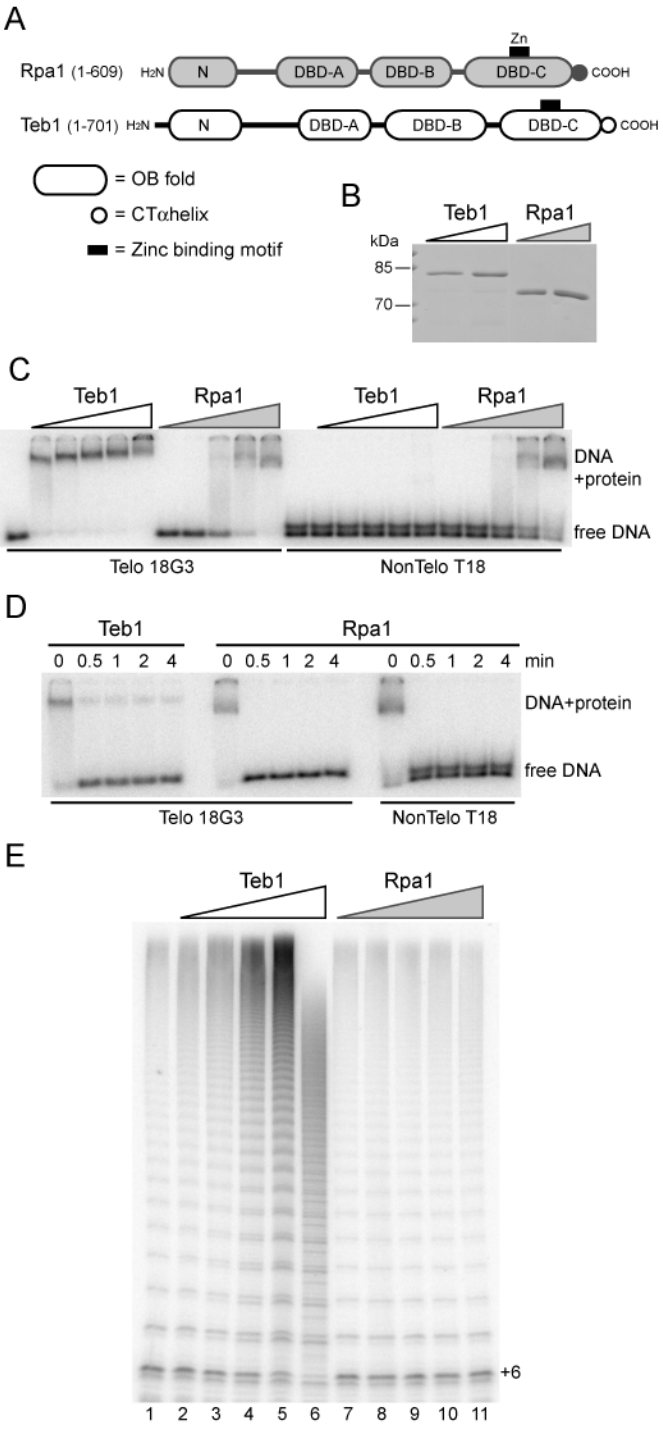
A
Rpa1 (1-609)
H2N
N
DBD-A
DBD-B
DBD-C
Zn
COOH
Teb1 (1-701)
= OB fold
= CTαhelix
= Zinc binding motif
B
Teb1
Rpa1
kDa
85
70
C
DNA
+protein
free DNA
Telo 18G3
NonTelo T18
D
0 0.5 1 2 4
min
DNA+protein
E
+6
1 2 3 4 5 6 7 8 9 10 11

Figure 2. Teb1 prefers longer and G_3T_2G permutation telomeric ssDNA.

(A) Permutation-dependent telomeric ssDNA-binding activity of Teb1. 10 pM probe was used with indicated amount of protein in gel shift assays.

(B) Length-dependence of Teb1 ssDNA-binding activity. 10 pM probe and 0.25-25.6 nM Teb1 was used in gel shift assays.

(C) Table of Kd calculations. The Kd measurements are an average of three independent experiments.

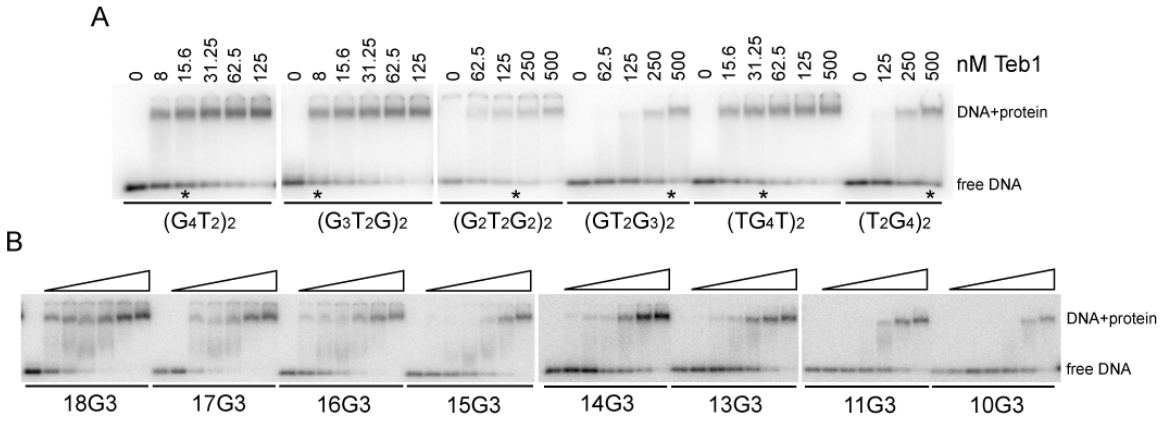

C

Name	Sequence	Kd (nM)
10G3	GGGTTGGGGT	16.4 ± 7.5
11G3	GGGTTGGGGTT	4.6 ± 2.1
12G3	GGGTTGGGGTTG	1.8 ± 0.45
13G3	GGGTTGGGGTTGG	3.9 ± 2.0
14G3	GGGTTGGGGTTGGG	1.74 ± 0.14
15G3	GGGTTGGGGTTGGGG	0.54 ± 0.41
16G3	GGGTTGGGGTTGGGGT	0.173 ± 0.11
17G3	GGGTTGGGGTTGGGGTT	0.037 ± 0.015
18G3	GGGTTGGGGTTGGGGTTG	0.025 ± 0.009

Figure 3. Telomerase holoenzyme with high RAP activity can be reconstituted with TERT, TER, TASC, and Teb1.

(A) Diagram of the components used for holoenzyme reconstitution.

(B) *T. thermophila* TASC purification. Silver-stained SDS-PAGE of telomerase and TASC purifications is shown.

(C) Reconstituted telomerase activity assay. High RAP activity is reconstituted only when both TASC and Teb1 are present, in addition to TERT and TER.

Figure 3

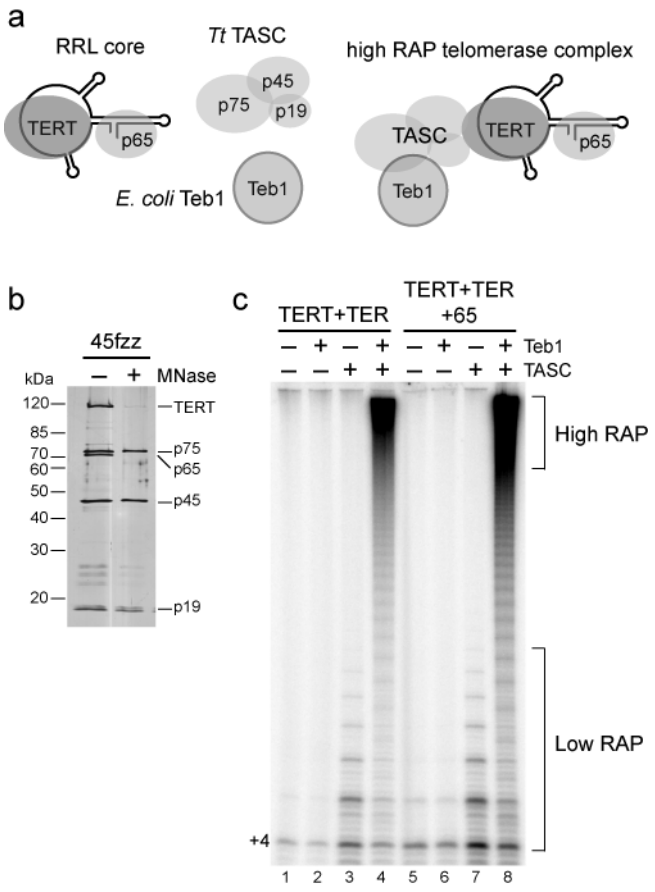
a
RRL core
TERT
p65
Tt TASC
p45
p75
p19
E. coli Teb1
Teb1
high RAP telomerase complex
TASC
TERT
p65
Teb1
b
45fzz
kDa
– + MNase
120
85
70
60
50
40
30
20
TERT
p75
p65
p45
p19
c
TERT+TER
TERT+TER
+65
– + – + – + – + Teb1
– – + + – – + + TASC
High RAP
Low RAP
+4
1 2 3 4 5 6 7 8

Figure 4. The A and B domains in Teb1 bind ssDNA and the C domain interacts with TASC.

(A) Diagram of Teb1 truncation constructs.

(B) Recombinant truncated Teb1 proteins.

(C) Telomeric ssDNA-binding activity of truncated Teb1 proteins. 20 nM 6FAM-$(T_2G_4)_3$ and 10-250 nM protein were used in gel shift assays.

(D) Teb1 truncation proteins in reconstituted telomerase activity assay. 200 nM 18G1 primer with 40 or 200 nM protein were used.

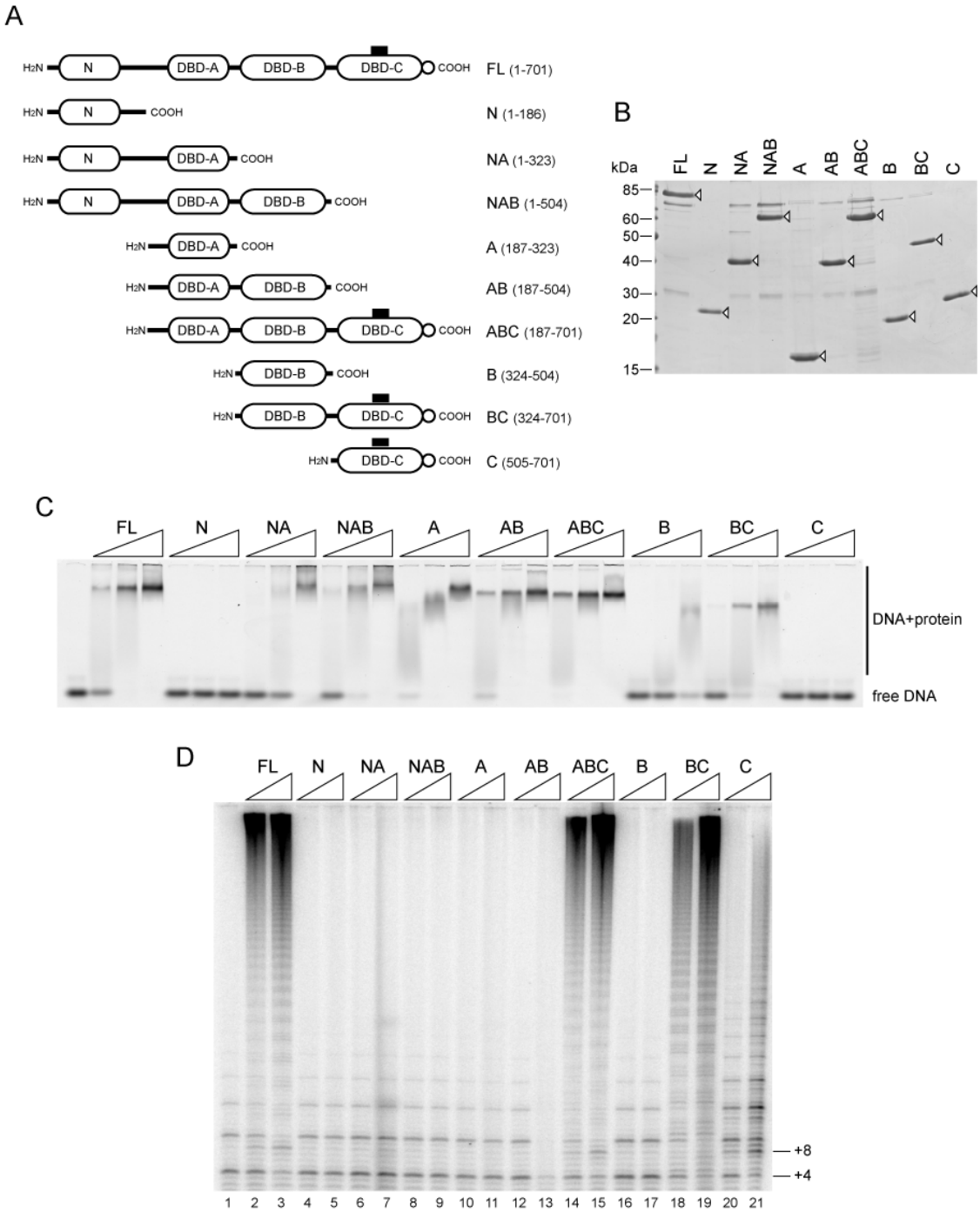
A
H2N
N
DBD-A
DBD-B
DBD-C
COOH
FL (1-701)
N (1-186)
NA (1-323)
NAB (1-504)
A (187-323)
AB (187-504)
ABC (187-701)
B (324-504)
BC (324-701)
C (505-701)
B
kDa
FL
N
NA
NAB
A
AB
ABC
B
BC
C
85
60
50
40
30
20
15
C
DNA+protein
free DNA
D
+8
+4
1 2 3 4 5 6 7 8 9 10 11 12 13 14 15 16 17 18 19 20 21

Figure 5. High RAP activity arises from the C domain of Teb1 connecting the ssDNA-binding activity to the holoenzyme.

(A) Diagram of mutant Teb1 proteins.

(B) Purified Teb1ΔCTαh and $Rpa1^{NAB}$-$Teb1^{C}$ recombinant proteins.

(C) ssDNA-binding activity of Teb1ΔCTαhelix and $Rpa1^{NAB}$-$Teb1^{C}$. 10 pM probe and 0.16-20 nM (Teb1ΔCTαh) or 0.16-500 nM $Rpa1^{NAB}$-$Teb1^{C}$ were used in gel shift assays.

(D) Teb1ΔCTαhelix and $Rpa1^{NAB}$-$Teb1^{C}$ proteins in reconstituted telomerase activity assay. 200 nM 18G1 primer with 40 or 100 nM protein were used.

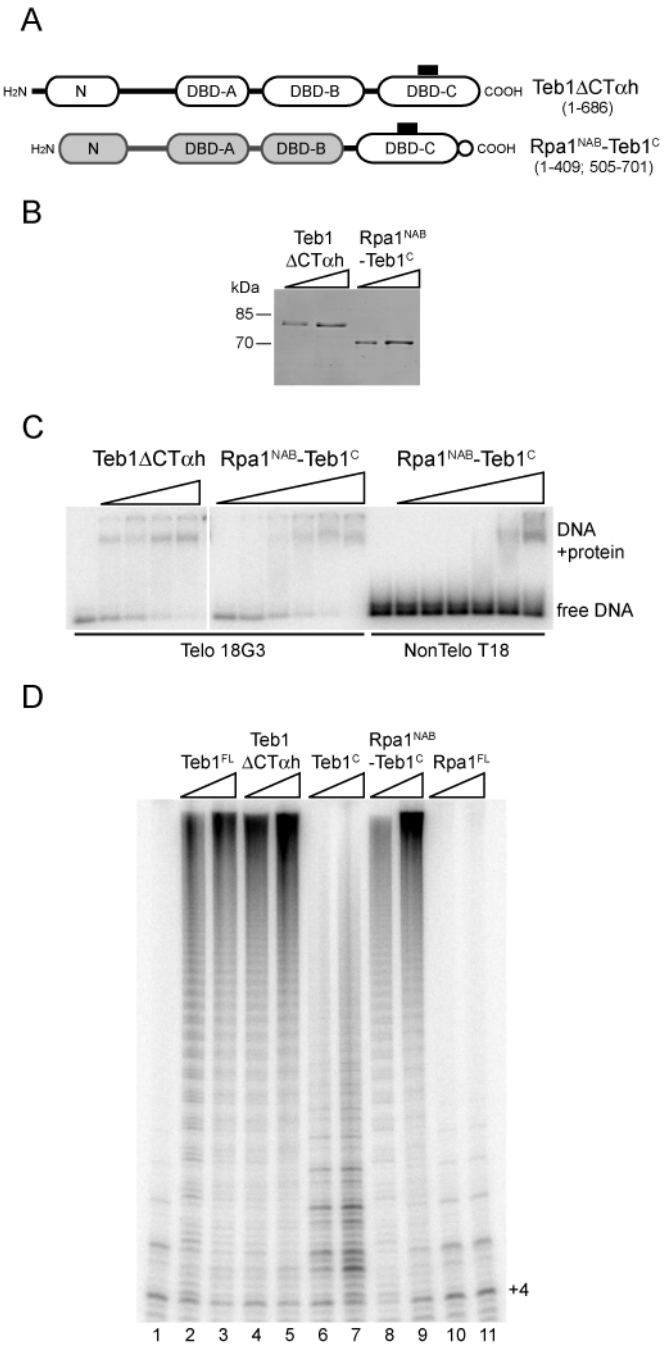
A
H2N
N
DBD-A
DBD-B
DBD-C
COOH
Teb1ΔCTαh
(1-686)
Rpa1NAB-Teb1C
(1-409; 505-701)
B
Teb1 ΔCTαh
Rpa1NAB -Teb1C
kDa
85
70
C
Teb1ΔCTαh
Rpa1NAB-Teb1C
DNA +protein
free DNA
Telo 18G3
NonTelo T18
D
Teb1FL
Teb1 ΔCTαh
Teb1C
Rpa1NAB -Teb1C
Rpa1FL
+4
1 2 3 4 5 6 7 8 9 10 11

Figure 6. Teb1 anchor site activity is coupled to telomerase holoenzyme through the interaction between the C domain and TASC.

Model of telomerase holoenzyme.

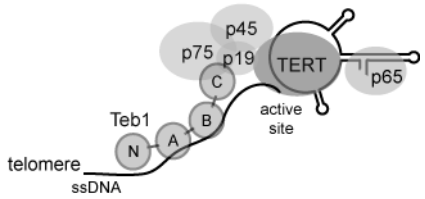
p45
p75
p19
TERT
p65
C
Teb1
B
active
site
N
A
telomere
ssDNA

REFERENCES

Avilion, A. A., Harrington, L. A., and Greider, C. W. (1992). Tetrahymena telomerase RNA levels increase during macronuclear development. Dev Genet *13*, 80-86.

Baumann, P., and Cech, T. R. (2001). Pot1, the putative telomere end-binding protein in fission yeast and humans. Science *292*, 1171-1175.

Bianchi, A., and Shore, D. (2008). How telomerase reaches its end: mechanism of telomerase regulation by the telomeric complex. Mol Cell *31*, 153-165.

Blackburn, E. H., Greider, C. W., and Szostak, J. W. (2006). Telomeres and telomerase: the path from maize, Tetrahymena and yeast to human cancer and aging. Nat Med *12*, 1133-1138.

Bochkarev, A., and Bochkareva, E. (2004). From RPA to BRCA2: lessons from single-stranded DNA binding by the OB-fold. Curr Opin Struct Biol *14*, 36-42.

Bochkareva, E., Korolev, S., Lees-Miller, S. P., and Bochkarev, A. (2002). Structure of the RPA trimerization core and its role in the multistep DNA-binding mechanism of RPA. EMBO J *21*, 1855-1863.

Casteel, D. E., Zhuang, S., Zeng, Y., Perrino, F. W., Boss, G. R., Goulian, M., and Pilz, R. B. (2009). A DNA polymerase-{alpha}{middle dot}primase cofactor with homology to replication protein A-32 regulates DNA replication in mammalian cells. J Biol Chem *284*, 5807-5818.

Chan, A., Boulé, J. B., and Zakian, V. A. (2008). Two pathways recruit telomerase to *Saccharomyces cerevisiae* telomeres. PLoS Genet *4*, e1000236.

Chandra, A., Hughes, T. R., Nugent, C. I., and Lundblad, V. (2001). Cdc13 both positively and negatively regulates telomere replication. Genes Dev *15*, 404-414.

Cohen, S., Jacob, E., and Manor, H. (2004). Effects of single-stranded DNA binding proteins on primer extension by telomerase. Biochim Biophys Acta *1679*, 129-140.

Collins, K. (1999). Ciliate telomerase biochemistry. Annu Rev Biochem *68*, 187-218.

Collins, K. (2006). The biogenesis and regulation of telomerase holoenzymes. Nat Rev Mol Cell Biol *7*, 484-494.

Collins, K. (2008). Physiological assembly and activity of human telomerase complexes. Mech Ageing Dev *129*, 91-98.

Collins, K. (2009). Forms and functions of telomerase RNA. In Non-Protein Coding RNAs, N. G. Walter, S. A. Woodson, and R. T. Batey, eds. (Berlin, Springer-Verlag), pp. 285-301.

Collins, K., and Greider, C. W. (1993). Nucleolytic cleavage and non-processive elongation catalyzed by *Tetrahymena* telomerase. Genes Dev *7*, 1364-1376.

Coyne, R. S., and al., e. (2008). Refined annotation and assembly of the *Tetrahymena thermophila* genome sequence through EST analysis, comparative genomic hybridization, and targeted gap closure. BMC Genomics *in press*.

Cristofari, G., Lingner, J. (2006). The Telomerase Ribonucleoprotein Particle, 2 edn (Cold Spring Harbor, Cold Spring Harbor Laboratory Press).

Croy, J. E., and Wuttke, D. S. (2006). Themes in ssDNA recognition by telomere-end protection proteins. Trends Biochem Sci *31*, 516-525.

Cunningham, D. D., and Collins, K. (2005). Biological and biochemical functions of RNA in the tetrahymena telomerase holoenzyme. Mol Cell Biol *25*, 4442-4454.

Eisen, J. A., and al., e. (2006). Macronuclear genome sequence of the ciliate *Tetrahymena thermophila*, a model eukaryote. PLoS Biol *4*, 1620-1642.
Errington, T. M., Fu, D., Wong, J. M., and Collins, K. (2008). Disease-associated human telomerase RNA variants show loss of function for telomere synthesis without dominant-negative interference. Mol Cell Biol *28*, 6510-6520.
Fisher, T. S., Taggart, A. K., and Zakian, V. A. (2004). Cell cycle-dependent regulation of yeast telomerase by Ku. Nat Struct Mol Biol *11*, 1198-1205.
Forsyth, N. R., Wright, W. E., and Shay, J. W. (2002). Telomerase and differentiation in multicellular organisms: turn it off, turn it on, and turn it off again. Differentiation *69*, 188-197.
Fu, D., and Collins, K. (2007). Purification of human telomerase complexes identifies factors involved in telomerase biogenesis and telomere length regulation. Mol Cell *28*, 773-785.
Gallardo, F., and Chartrand, P. (2008). Telomerase biogenesis: The long road before getting to the end. RNA Biol *5*, 212-215.
Gallardo, F., Olivier, C., Dandjinou, A. T., Wellinger, R. J., and Chartrand, P. (2008). TLC1 RNA nucleo-cytoplasmic trafficking links telomerase biogenesis to its recruitment to telomeres. EMBO J *27*, 748-757.
Gao, H., Cervantes, R. B., Mandell, E. K., Otero, J. H., and Lundblad, V. (2007). RPA-like proteins mediate yeast telomere function. Nat Struct Mol Biol *14*, 208-214.
Gelinas, A. D., Paschini, M., Reyes, F. E., Heroux, A., Batey, R. T., Lundblad, V., and Wuttke, D. S. (2009). Telomere capping proteins are structurally related to RPA with an additional telomere-specific domain. Proc Natl Acad Sci U S A *106*, 19298-19303.
Gilson, E., and Geli, V. (2007a). How telomeres are replicated. Nat Rev Mol Cell Biol *8*, 825-838.
Gilson, E., and Geli, V. (2007b). How telomeres are replicated. Nat Rev Mol Cell Biol *8*, 825-838.
Gomes, X. V., and Wold, M. S. (1996). Functional domains of the 70-kilodalton subunit of human replication protein A. Biochemistry *35*, 10558-10568.
Gottschling, D. E., and Zakian, V. A. (1986). Telomere proteins: specific recognition and protection of the natural termini of Oxytricha macronuclear DNA. Cell *47*, 195-205.
Greider, C. W. (1991). Telomerase is processive. Mol Cell Biol *11*, 4572-4580.
Greider, C. W., and Blackburn, E. H. (1985). Identification of a specific telomere terminal transferase activity in Tetrahymena extracts. Cell *43*, 405-413.
Hardy, C. D., Schultz, C. S., and Collins, K. (2001). Requirements for the dGTP-dependent repeat addition processivity of recombinant *Tetrahymena* telomerase. J Biol Chem *276*, 4863-4871.
Haring, S. J., and Wold, M. S. (2007). A common means to an end. Nat Struct Mol Biol *14*, 176-177.
Horvath, M. P., Schweiker, V. L., Bevilacqua, J. M., Ruggles, J. A., and Schultz, S. C. (1998). Crystal structure of the *Oxytricha nova* telomere end binding protein complexed with single strand DNA. Cell *95*, 963-974.
Iftode, C., Daniely, Y., and Borowiec, J. A. (1999). Replication protein A (RPA): the eukaryotic SSB. Crit Rev Biochem Mol Biol *34*, 141-180.

Jacob, N. K., Lescasse, R., Linger, B. R., and Price, C. M. (2007). Tetrahymena POT1a regulates telomere length and prevents activation of a cell cycle checkpoint. Mol Cell Biol *27*, 1592-1601.
Jacob, N. K., Skopp, R., and Price, C. M. (2001). G-overhang dynamics at *Tetrahymena* telomeres. EMBO J *20*, 4299-4308.
Kibe, T., Ono, Y., Sato, K., and Ueno, M. (2007). Fission yeast Taz1 and RPA are synergistically required to prevent rapid telomere loss. Mol Biol Cell *18*, 2378-2387.
Lee, M. S., and Blackburn, E. H. (1993). Sequence-specific DNA primer effects on telomerase polymerization activity. Mol Cell Biol *13*, 6586-6599.
Lee, S. R., and Collins, K. (2007). Physical and functional coupling of RNA-dependent RNA polymerase and Dicer in the biogenesis of endogenous siRNAs. Nat Struct Mol Biol *14*, 604-610.
Li, S., Makovets, S., Matsuguchi, T., Blethrow, J. D., Shokat, K. M., and Blackburn, E. H. (2009). Cdk1-dependent phosphorylation of Cdc13 coordinates telomere elongation during cell-cycle progression. Cell *136*, 50-61.
Lingner, J., Cech, T. R., Hughes, T. R., and Lundblad, V. (1997). Three ever shorter telomere (*EST*) genes are dispensable for in vitro yeast telomerase activity. Proc Natl Acad Sci USA *94*, 11190-11195.
Lue, N. F. (2009). Closing the feedback loop: how cells "count" telomere-bound proteins. Mol Cell *33*, 413-414.
Miao, W., Xiong, J., Bowen, J., Wang, W., Liu, Y., Braguinets, O., Grigull, J., Pearlman, R. E., Orias, E., and Gorovsky, M. A. (2009). Microarray analyses of gene expression during the *Tetrahymena thermophila* life cycle. PLoS ONE *4*, e4429.
Miller, K. M., Rog, O., and Cooper, J. P. (2006). Semi-conservative DNA replication through telomeres requires Taz1. Nature *440*, 824-828.
Miller, M. C., and Collins, K. (2000). The *Tetrahymena* p80/p95 complex is required for proper telomere length maintenance and micronuclear genome stability. Mol Cell *6*, 827-837.
Min, B., Collins, K. (2009). An RPA-related Sequence-Specific DNA-Binding Subunit of Telomerase Holoenzyme is Required for Elongation Processivity and Telomere Maintenance. Molecular Cell.
Miyake, Y., Nakamura, M., Nabetani, A., Shimamura, S., Tamura, M., Yonehara, S., Saito, M., and Ishikawa, F. (2009). RPA-like mammalian Ctc1-Stn1-Ten1 complex binds to single-stranded DNA and protects telomeres independently of the Pot1 pathway. Mol Cell *36*, 193-206.
Miyoshi, T., Kanoh, J., Saito, M., and Ishikawa, F. (2008). Fission yeast Pot1-Tpp1 protects telomeres and regulates telomere length. Science *320*, 1341-1344.
Moser, B. A., and Nakamura, T. M. (2009). Protection and replication of telomeres in fission yeast. Biochem Cell Biol *87*, 747-758.
Neto, J. L., Lira, C. B., Giardini, M. A., Khater, L., Perez, A. M., Peroni, L. A., dos Reis, J. R., Freitas-Junior, L. H., Ramos, C. H., and Cano, M. I. (2007). Leishmania replication protein A-1 binds in vivo single-stranded telomeric DNA. Biochem Biophys Res Commun *358*, 417-423.
Nugent, C. I., Hughes, T. R., Lue, N. F., and Lundblad, V. (1996). Cdc13p: a single-strand telomeric DNA-binding protein with a dual role in yeast telomere maintenance. Science *274*, 249-252.

O'Connor, C. M., and Collins, K. (2006). A novel RNA binding domain in *Tetrahymena* telomerase p65 initiates hierarchical assembly of telomerase holoenzyme. Mol Cell Biol *26*, 2029-2036.
Oganesian, L., and Karlseder, J. (2009). Telomeric armor: the layers of end protection. J Cell Sci *122*, 4013-4025.
Osterhage, J. L., Talley, J. M., and Friedman, K. L. (2006). Proteasome-dependent degradation of Est1p regulates the cell cycle-restricted assembly of telomerase in *Saccharomyces cerevisiae*. Nat Struct Mol Biol *13*, 720-728.
Palm, W., and de Lange, T. (2008). How shelterin protects mammalian telomeres. Annu Rev Genet *42*, 301-334.
Pennock, E., Buckley, K., and Lundblad, V. (2001). Cdc13 delivers separate complexes to the telomere for end protection and replication. Cell *104*, 387-396.
Prathapam, R., Witkin, K. L., O'Connor, C. M., and Collins, K. (2005). A telomerase holoenzyme protein enhances telomerase RNA assembly with telomerase reverse transcriptase. Nat Struct Mol Biol *12*, 252-257.
Price, C. M., and Cech, T. R. (1987). Telomeric DNA-protein interactions of Oxytricha macronuclear DNA. Genes Dev *1*, 783-793.
Qi, H., and Zakian, V. A. (2000). The Saccharomyces telomere-binding protein Cdc13p interacts with both the catalytic subunit of DNA polymerase alpha and the telomerase-associated est1 protein. Genes Dev *14*, 1777-1788.
Ray, S., Karamysheva, Z., Wang, L., Shippen, D. E., and Price, C. M. (2002). Interactions between telomerase and primase physically link the telomere and chromosome replication machinery. Mol Cell Biol *22*, 5859-5868.
Rubtsova, M. P., Skvortsov, D. A., Petruseva, I. O., Lavrik, O. I., Spirin, P. V., Prasolov, V. S., Kisseljov, F. L., and Dontsova, O. A. (2009). Replication protein A modulates the activity of human telomerase in vitro. Biochemistry (Mosc) *74*, 92-96.
Salas, T. R., Petruseva, I., Lavrik, O., Bourdoncle, A., Mergny, J. L., Favre, A., and Saintome, C. (2006). Human replication protein A unfolds telomeric G-quadruplexes. Nucleic Acids Res *34*, 4857-4865.
Schramke, V., Luciano, P., Brevet, V., Guillot, S., Corda, Y., Longhese, M. P., Gilson, E., and Géli, V. (2004). RPA regulates telomerase action by providing Est1p access to chromosome ends. Nat Genet *36*, 46-54.
Shakirov, E. V., Surovtseva, Y. V., Osbun, N., and Shippen, D. E. (2005). The Arabidopsis Pot1 and Pot2 proteins function in telomere length homeostasis and chromosome end protection. Mol Cell Biol *25*, 7725-7733.
Shang, Y., Song, X., Bowen, J., Corstanje, R., Gao, Y., Gaertig, J., and Gorovsky, M. A. (2002). A robust inducible-repressible promoter greatly facilitates gene knockouts, conditional expression, and overexpression of homologous and heterologous genes in *Tetrahymena thermophila*. Proc Natl Acad Sci USA *99*, 3734-3739.
Stellwagen, A. E., Haimberger, Z. W., Veatch, J. R., and Gottschling, D. E. (2003). Ku interacts with telomerase RNA to promote telomere addition at native and broken chromosome ends. Genes Dev *17*, 2384-2395.
Stone, M. D., Mihalusova, M., O'Connor C, M., Prathapam, R., Collins, K., and Zhuang, X. (2007). Stepwise protein-mediated RNA folding directs assembly of telomerase ribonucleoprotein. Nature *446*, 458-461.

Surovtseva, Y. V., Churikov, D., Boltz, K. A., Song, X., Lamb, J. C., Warrington, R., Leehy, K., Heacock, M., Price, C. M., and Shippen, D. E. (2009). Conserved telomere maintenance component 1 interacts with STN1 and maintains chromosome ends in higher eukaryotes. Mol Cell *36*, 207-218.
Teixeira, M. T., and Gilson, E. (2007). La sets the tone for telomerase assembly. Nat Struct Mol Biol *14*, 261-262.
Venteicher, A. S., Abreu, E. B., Meng, Z., McCann, K. E., Terns, R. M., Veenstra, T. D., Terns, M. P., and Artandi, S. E. (2009). A human telomerase holoenzyme protein required for Cajal body localization and telomere synthesis. Science, 644-648.
Wang, F., Podell, E. R., Zaug, A. J., Yang, Y., Baciu, P., Cech, T. R., and Lei, M. (2007). The POT1-TPP1 telomere complex is a telomerase processivity factor. Nature *445*, 506-510.
Witkin, K. L., and Collins, K. (2004). Holoenzyme proteins required for the physiological assembly and activity of telomerase. Genes Dev *18*, 1107-1118.
Witkin, K. L., Prathapam, R., and Collins, K. (2007). Positive and negative regulation of Tetrahymena telomerase holoenzyme. Mol Cell Biol *27*, 2074-2083.
Wold, M. S. (1997). Replication protein A: a heterotrimeric, single-stranded DNA-binding protein required for eukaryotic DNA metabolism. Annu Rev Biochem *66*, 61-92.
Xin, H., Liu, D., Wan, M., Safari, A., Kim, H., Sun, W., O'Connor, M. S., and Songyang, Z. (2007). TPP1 is a homologue of ciliate TEBP-beta and interacts with POT1 to recruit telomerase. Nature *445*, 559-562.
Yu, G., and Blackburn, E. H. (1991). Developmentally programmed healing of chromosomes by telomerase in *Tetrahymena*. Cell *67*, 823-832.